Journal of Medicinal Chemistry

Article

Potent anti-glioblastoma agents by hybridizing the onium-alkyloxy-stilbene based structures of an alpha7-, alpha9-nAChR antagonist and of a pro-oxidant mitocan

francesco bavo, susanna pucci, francesca fasoli, Carmen Lammi, milena moretti, vanessa mucchietto, donatella lattuada, paola viani, clara de palma, Roberta Budriesi, irene corradini, Cheryl Dowell, J. Michael McIntosh, francesco clementi, Cristiano Bolchi, cecilia gotti, and Marco Pallavicini

J. Med. Chem., **Just Accepted Manuscript** • DOI: 10.1021/acs.jmedchem.8b01052 • Publication Date (Web): 07 Nov 2018

Just Accepted

ACS Publications

is published by the American Chemical Society. 1155 Sixteenth Street N.W., Washington, DC 20036

Potent anti-glioblastoma agents by hybridizing the onium-alkyloxy-stilbene based structures of an α7-, α9-nAChR antagonist and of a pro-oxidant mitocan

Francesco Bavo[1°], Susanna Pucci[2°], Francesca Fasoli[2°], Carmen Lammi[1], Milena Moretti[2,3], Vanessa Mucchietto[2], Donatella Lattuada[3], Paola Viani[3], Clara De Palma[4], Roberta Budriesi[5], Irene Corradini[2], Cheryl Dowell[6], J. Michael McIntosh[6,7,8], Francesco Clementi[2,3], Cristiano Bolchi[1*], Cecilia Gotti[2,3*], and Marco Pallavicini[1]

[1]*Dipartimento di Scienze Farmaceutiche , Università degli Studi di Milano, Via Mangiagalli 25, I-20133, Milano, Italy*

[2]*CNR, Institute of Neuroscience, Via Vanvitelli 32, I-20129, Milano, Italy*

[3]*Department of Medical Biotechnology and Translational Medicine, Università degli Studi di Milano, Via Vanvitelli 32, I-20129, Milano, Italy*

[4]*Unit of Clinical Pharmacology, University Hospital "Luigi Sacco"-ASST Fatebenefratelli Sacco, Via G. B. Grassi 74, I-20157, Milano, Italy*

[5]*Dipartimento di Farmacia e Biotecnologie, Università degli Studi di Bologna, Via Belmeloro 6, I-40126, Bologna, Italy*

[6] *Department of Biology University of Utah, 257S.1400 East, Salt Lake City, UT 84112, USA.*

[7]*George E. Wahlen Veterans Affairs Medical Center, 500 Foothill Drive, Salt Lake City, UT 84148, USA.*

[8]*Department of Psychiatry, University of Utah, 501 Chipeta Way, Salt Lake City, Ut 84108, USA*

° Co-first authors

*Co-corresponding authors

Abstract

Adenocarcinoma and glioblastoma cell lines express α7 and α9-α10-containing nAChRs, whose activation promotes tumour cells growth. On these cells, the triethylammoniumethyl ether of 4-stilbenol MG624, a known selective antagonist of α7 and α9-α10 nAChRs, has antiproliferative activity. The structural analogy of MG624 with the mitocan RDM-4'BTPI, triphenylphosphoniumbutyl ether of pterostilbene, suggested us that molecular hybridisation among their three substructures (stilbenoxy residue, alkylene linker and terminal onium) and elongation of the alkylene linker might result in novel antitumour agents with higher potency and selectivity. We found that lengthening the ethylene bridge in the triethylammonium derivatives results in more potent and selective toxicity towards adenocarcinoma and glioblastoma cells, which was paralleled by increased α7 and α9-α10 nAChR antagonism and improved ability of reducing mitochondrial ATP production. Elongation of the alkylene linker was advantageous also for the triphenylphosphonium derivatives resulting in a generalized enhancement of antitumor activity, associated with increased mitotoxicity.

INTRODUCTION

Since 2000, a considerable number of reports have suggested that cancer cells, compared to their non-tumoral counterparts, are characterized by altered redox homeostasis and hyperpolarized inner mitochondrial membrane (IMM). [1,2] Permanently enhanced production of Reactive Oxygen Species (ROS) by mitochondria may predispose to carcinogenesis, tumor growth and metastasis, but, on the other hand, sudden, notable and targeted ROS enhancement can activate pro-apoptotic signaling and induce Mitochondrial Permeability Transition (MPT) resulting in cell death. [3] These observations have suggested that the antitumor potential of substances increasing ROS production, such as resveratrol at high doses, quercetin and α-tocopheryl succinate, can be maximized if the compounds

are targeted to mitochondrial matrix, with preference for the hyperpolarized mitochondria of cancer cells, by coupling to a membrane-permeable lipophilic cation.[4] Connection to a triphenylphosphonium head, a charged but lipophilic moiety, through an alkylene linker is the most widely used strategy to make these molecules 'mitochondriotropic'. MitoVES,[5] Q-7BTPI [6] and, more recently, the 3',5'-dimethoxy-4-stilbenol (pterostilbene) derivative RDM-4'BTPI from now on defined **PtP-4** [7] are successful examples of mitochondria-targeted cytotoxic pro-oxidants, classified within the so-called 'mitocans' (Chart 1).

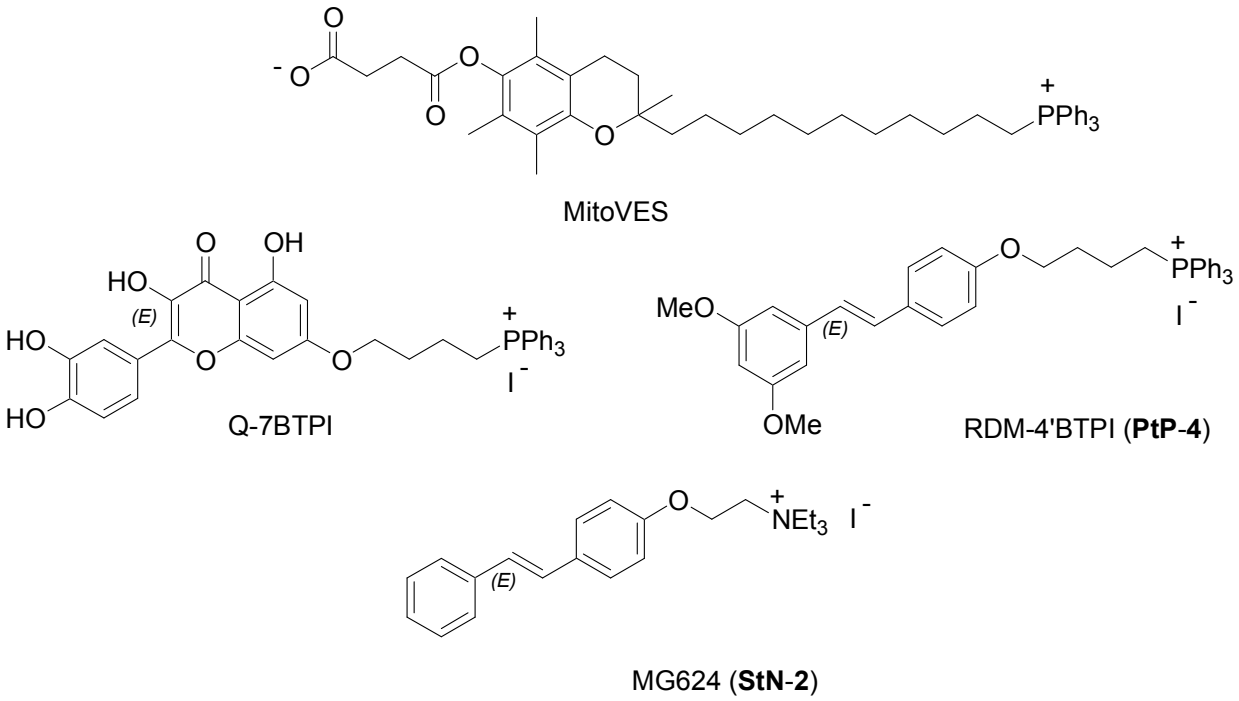

Chart 1. Cytotoxic pro-oxidants targeted to mitochondria by triphenylphosphonium head and the stilbenoxyethylammonium α7 and α9 nAChR antagonist MG624.

Our attention was drawn to RDM-4'BTPI and to some analogies between its structure and that of MG624 from now on defined **StN-2** , an antagonist of the α7 and α9 neuronal nicotinic acetylcholine receptors (nAChRs) that we developed in 1998 (Chart 1).[8] nAChRs are ligand-gated ion channels widely distributed throughout the central and peripheral nervous systems, [9] that also have an extraneuronal localisation. [10] In particular, the subtypes containing the α7 or the α9 subunits are

present in endothelial cells, glia, immune cells, lung epithelia and cancer cells, where they regulate cell differentiation, proliferation and inflammatory responses. [11,12] Recently, we characterized **StN-2** for its ability to increase ROS production and to block the α7 and α9 nAChR mediated pro-proliferative effect of nicotine in pulmonary adenocarcinoma cells. [13] The two molecules, **PtP-4** and **StN-2**, share a stilbene scaffold with a *para* positioned quaternary ω-onium alkyloxy residue, four and two carbons long respectively, and both behave as cytotoxic pro-oxidants. Furthermore, SAR studies on regioisomeric resveratrol 4-triphenylphosphoniumbutyl ethers as mitocans proved that methylation of the two remaining free hydroxyls, both meta positioned on the same phenyl (**PtP-4**) or meta and para separately positioned on the two phenyls, resulted in highly increased cytotoxicity due to ROS generation. [7] This indicated that, at variance with mitochondriotropic derivatives of quercetin, free hydroxyls are not essential for the activity of mitochondriotropic resveratrol derivatives and suggested that the two methoxy functions could be removed by switching to the unsubstituted stilbene scaffold.

Based on these premises, we planned a systematic hybridization between the three constitutive portions of **PtP-4** (pterostilbene residue (**Pt**), triphenylphosphonium head (**P**) and **4**C linker) and of **StN-2** (stylbenoxy residue (**St**), triethylammonium head (**N**) and **2**C linker) and a biological characterization of the resultant series of eight phosphonium and ammonium iodides. These are shown in Chart 2 and identified with a code composed of the initials of the name of the aromatic scaffold (**Pt** for pterostilbene and **St** for stilbene), the onium head hetero atom (**P** or **N**), followed by the number of the linker carbons. In particular, we wished to test their anti-proliferative activity on different tumor cells expressing α7 and /or α9 nAChRs and to analyze the underlying mechanisms. In this way, we hoped to understand the role played by the three substructures (onium head, stilbene scaffold and interposed alkylene linker) in addressing the activity towards one or more biological targets and to find advantageous synergies between different mechanisms.

Furthermore, we were particularly interested in the elongation of the alkylene linker, a structural modification expected to be relevant to both nicotinic antagonism, for the increase of steric

encumbrance, and cytotoxic pro-oxidant activity. Useful information would have been gained from α7 and α9 nAChR antagonism comparison between **PtN-2** and its two-carbon-elongated analogue **PtN-4** and between **StN-2** and the elongated **StN-4**, **StN-6** and **StN-8** analogues, while a further elongation of the butylene linker of **PtP-4** was strongly suggested by evidences from the literature. In fact, **PtP-4** has been suggested to act as mitoVES, whose activity has been reported to be diminished by shortening its eleven-carbon long linker. [14] Consistently with such a trend, elongation of the short 4 C linker of **StP-4**, the stilbene analogue of **PtP-4**, could be beneficial. Therefore, we extended the series of compounds to be investigated over the stilbenoxyalkyl triphenylphosphonium iodides **PtP-3** and **PtP-5-PtP-10** having alkylene linkers of increasing length.

Here, we report the synthesis of the compounds shown in Chart 2, except for the previously described **StN-2** (MG624) and **PtP-4** (RDM-4'BTPI), and discuss their pharmacological activity and those of MG624 and RDM-4'BTPI comparing their profiles as antiproliferative agents against glioblastoma, other tumor cells and normal glial cells (astrocytes) and analysing their behaviour as α7 and α9 nAChR ligands and cytotoxic pro-oxidants. Unfortunately, compounds with two-carbon linker and phosphonium head, **PtPt-2** and **StP-2**, could not be enclosed into this investigation because ready decomposition to pterostilbene and stilbenol, respectively, and vinyl-triphenylphosphonium precluded their isolation and characterization.[15]

Chart 2. Target phosphonium and ammonium compounds resulting from hybridization between MG624 (**StN-2**) and RDM-4'BTPI (**PtP-4**) and from alkylene linker elongation.

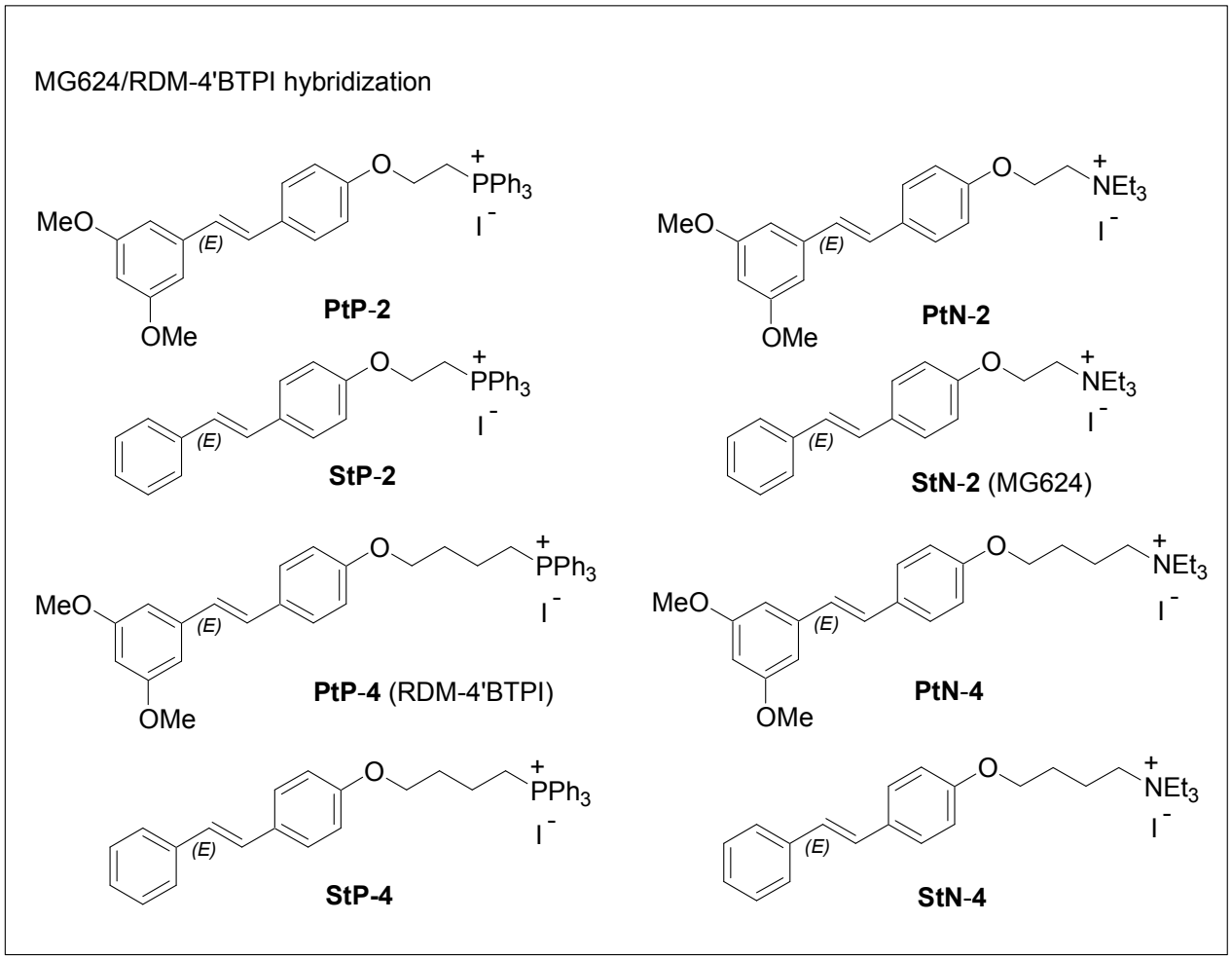

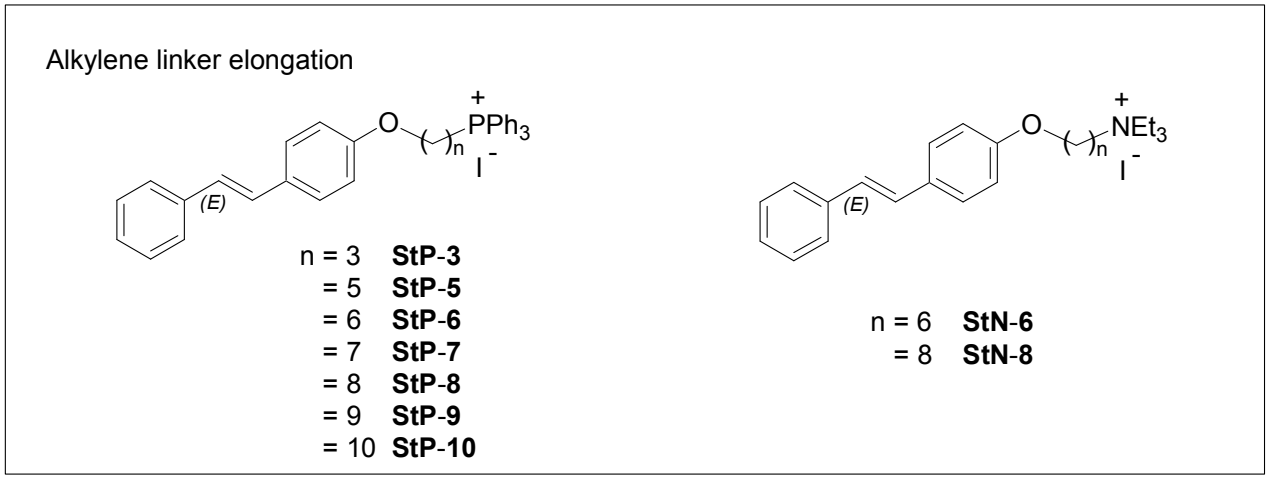

RESULTS

Chemistry

The pterostilbene ammoniumalkyl ethers **PtN-2** and **PtN-4** were synthesized from commercial resveratrol, while the stilbenol ammoniumalkyl ethers **StN-4**, **StN-6** and **StN-8** and the eight stilbenol phosphoniumalkyl ethers **StP-3 – StP-10** from commercial 4-(*E*)-stilbenol (Scheme 1). Alkylation of resveratrol with 1-bromo-2-choloroethane and 1-bromo-4-chlorobutane afforded, respectively, the intermediates **1a** and **1c**, whose free phenolic functions were methylated to obtain the O-chloroalkyl pterostilbene intermediates **2a** and **2c**. These were converted into the corresponding iodoalkyl analogues **3a** and **3c** by Finkelstein reaction and then into the final triethylammonium derivatives **PtN-2** and **PtN-4** by treatment with triethylamine. The ethers with stilbene scaffold were synthesized by the same strategy but using α,ω-dibromoalkanes to O-alkylate 4-(*E*)-stilbenol. The resulting ω-bromoalkyl ethers **4b-i** were converted into the corresponding ω-iodoalkyl ethers **5b-i**. Reaction of **5c**, **5e** and **5g** with triethylamine afforded the triethylammonium derivatives **StN-4**, **StN-6** and **StN-8**, while reaction of **5b-i** with triphenylphosphine the corresponding triphenylphosphonium derivatives **StP-3-10**. RDM-4'BTPI (**PtP-4**) and **StN-2** (MG624) were synthesized as previously reported. [7,8]

Scheme 1

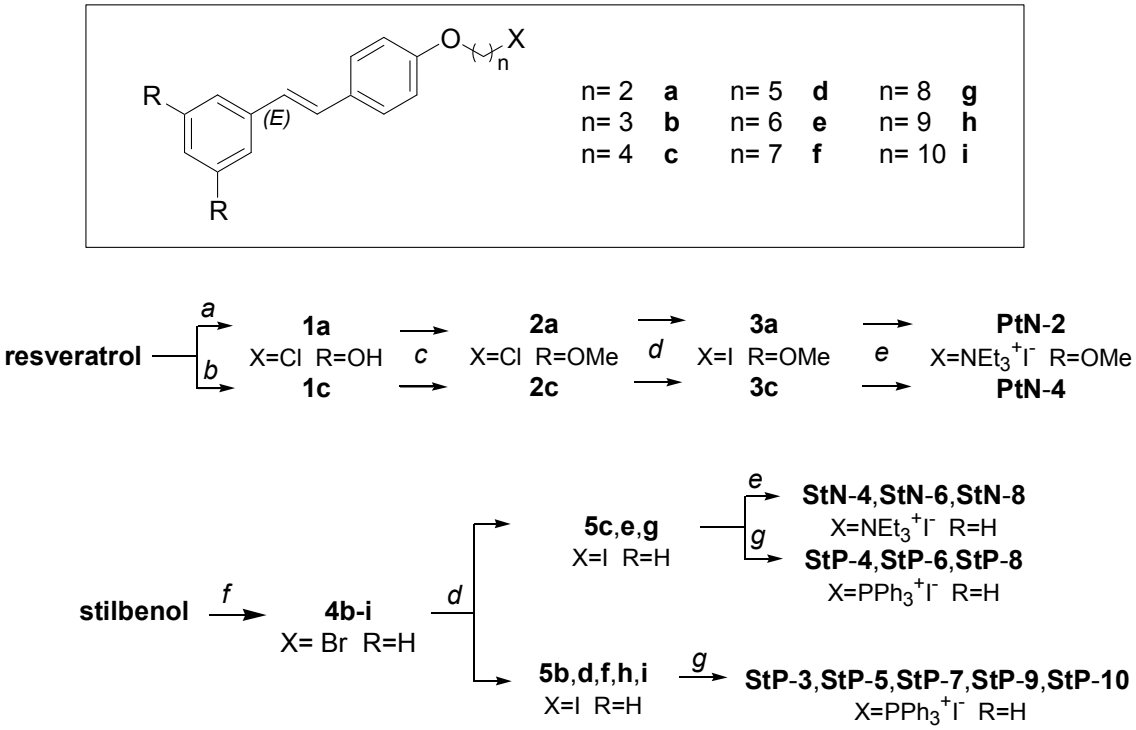

Reagents and conditions: (*a*) 1-bromo-2-chloroethane, K_2CO_3, DMF, 60 °C, overnight; (*b*) 1-bromo-4-chlorobutane, K_2CO_3, DMF, 60 °C, overnight; (*c*) MeI, $CsCO_3$, DMF, rt, overnight; (*d*) NaI sat. in acetone, reflux, overnight; (e) NEt_3, toluene, reflux, 5 h; (*f*) 1,3-dibromopropane (**4b**) or 1,4-dibromobutane (**4c**) or 1,5-dibromopentane (**4d**) or 1,6-dibromohexane (**4e**) or 1,7-dibromoheptane (**4f**) or 1,8-dibromooctane (**4g**) or 1,9-dibromononane (**4h**) or 1,10-dibromodecane (**4i**), NaOH, DMSO, rt, 3h; (*g*) PPh_3, neat, 100 °C, 3 h.

Biology

Binding studies

We tested the affinity of the synthesized compounds for the human α4β2 or α7 subtypes expressed in heterologous cells respectively labeled by [^{3}H]-Epibatidine or [^{125}I]-αBungarotoxin. Compounds **PtN-2**, **StN-2**, **StN-4**, and **StN-8** had very similar α7 affinities ranging from 100 to 200 nM Ki,

whereas **PtN-4** and **StN-6** had slightly lower affinities (305 nM and 465 nM). All of the phosphonium compounds had low α7 affinities that were approximately 6-10 times lower than that of **StN-2** (see Tables 1 and 2). When tested on the α4β2 subtypes, all of the ammonium compounds showed very similar α4β2 low affinities (Ki > 3 μM) (data not shown).

***In vitro* functional activity on α7 and α9α10 nAChR subtypes**

We have previously shown that **StN-2** is a selective antagonist of the human α7 and α9α10 nicotinic subtypes expressed in oocytes[13], and so we tested the new compounds using the same expression system and subtypes. Table 1 shows the potency of all of the ammonium compounds in inhibiting 10 μM or 200 μM ACh-induced currents in oocytes expressing the human α9α10 and α7 subtypes. Their IC_{50} values were all <100 nM. Increasing the linker length of **StN-2** (compounds **StN-4** and **StN-6**) increased antagonist potency against both subtypes, whereas **StN-8** was more active on α9α10. We also tested the possible antagonist activity of **PtP-4** on the α7 and α9α10 subtypes and found that the IC_{50} was > than 10 μM.

Effect of ammonium and phosphonium compounds on tumoral cells and normal astrocyte viability

The cytotoxic/cytostatic action of nine compounds (the six ammoniums **PtN-2**, **StN-2**, **PtN-4** , **StN-4**, **StN-6** and **StN-8** and the three phosphoniums **PtP-4**, **StP-4** and **StP-10**) was tested using MTS assays on U87MG glioblastoma, A549 adenocarcinoma, SH-SY5Y neuroblastoma cell lines and wild-type mouse astrocytes. All of the tumor cells and control astrocytes were incubated with increasing concentrations of the compounds for 72 h, and their activity was tested taking the absorbance of the control cells (not treated with the compounds) as 100%. The dose–response curves were fitted by means of non-linear regression analysis, and the concentration that blocked 50% of the viability (IC_{50}) was determined.

Table 1. Pharmacological and biological characterisation of the ammonium and phosphonium compounds

Cpd	Affinity[a] α7 receptors K_i, nM (CI)	Oocyte-expressed[b] α7 IC_{50},nM (CI)	Oocyte-expressed[b] α9α10 IC_{50},nM (CI)	Viability[c] IC_{50},μM U87MG 72h	Viability[c] IC_{50} μM A549 72h	Viability[c] IC_{50},μM SH-SY5Y 72h	Viability[c] IC_{50},μM mouse astrocytes 72h
StN-2 MG624	**104** (54-202)	**41** (20-72)	**10** (8-13.4)	**4.4**	**4.7**	**>100**	**47**
PtN-2	**189** (96-373)	**47** (30-74)	**17.2** (7-41)	**5.3**	**12**	**>100**	**23**
PtN-4	**305** (69-1356)	**24.3** (15-39)	**11.9** (7.3-19.4)	**0.57**	**3.3**	**11**	**22**
StN-4	**186** (80-433)	**6.5** (4.5-9.4)	**5** (3.8-6.4)	**1.8**	**3.5**	**31**	**20**
StN-6	**465** (168-1291)	**12.3** (7.7-19.5)	**4.8** (3.9-5.8)	**3.9**	**3.6**	**30**	**5.8**
StN-8	**164** (44-619)	**92** (67-125)	**6.6** (5.2-8.6)	**0.11**	**0.49**	**10**	**2**
PtP-4 RDM-4'BTPI	**1826** (830-4017)	**>10000**	**>10000**	**0.86**	**0.26**	**0.55**	**1**
StP-4	**1638** (617-4342)	Not done	Not done	**0.64**	**0.42**	**3.0**	**0.4**
StP-10	**1930** (587-6336)	Not done	Not done	**0.06**	**0.10**	**0.21**	**0.6**

[a] The affinity (K_i) for the human α7 subtype ammoniums MG624, PtN-2, PtN-4 , StN-4, StN-6 and StN-8 and the phosphoniums RDM-4'BTPI, StP-4 and StP-10 was tested in 3-4 independent competition binding experiments using [^{125}I]- αBungarotoxin and the transfected α7 subtype. CI=confidence interval of the K_i.

[b] All of the ammonium compounds and RDM-4'BTPI were functionally tested. In order to obtain concentration response data concerning their inhibitory effects, concentrations between 0.01 nM and 100 μM were co-applied with 10 μM ACh (α9α10 nAChR) or 200 μM ACh (α7 nAChR) and the peak current responses were normalized to the peak of the responses elicited by ACh alone; the normalized data were then fitted to the Hill equation using non-linear regression. Shown are the IC_{50} values and the confidence interval (CI) of the IC_{50}.

[c] The cytotoxic/cytostatic action of the nine compounds was tested using the MTS assays of three tumoral cell lines (U87MG glioblastoma, A549 adenocarcinoma and SH-SY5Y neuroblastoma) and wild type mice astrocytes. All of the cells were incubated with increasing concentrations for 72 h. The IC_{50} values were determined from the dose–response curves fitted using non- linear regression analysis, taking the absorbance of the control cells (not treated with compounds) as 100%.

As shown in Table 1, all the ammonium compounds, other than StN-8 , were less potent (higher IC_{50} values) than the phosphonium compounds, which were similarly potent against all of the tumoral and non-tumoral cells. Although less potent, the ammonium compounds were efficacious on U87MG and A549 cells, but not on SH-SY5Y cells or control astrocytes. In both ammonium and phosphonium series, the maximum potencies corresponded to the maximum linker length, eigth (**StN-8**) and ten methylenes (**PtP-10**) respectively, resulting in similar ≤ 100 nM IC_{50} values against U87MG glioblastoma and A549 adenocarcinoma. Table 2 shows the cytotoxic/cytostatic action of **StP-3** to **StP-10** on U87MG glioblastoma and A549 cell lines, the potency of which increased with the increasing length of the alkylene linker.

ATP production

We determined the ability of the nine compounds listed in Table 1 to interfere with ATP production by incubating them with U87MG cells for one or 72 hours. The tested concentrations were those determined by the MTS assay, which were in the range of the IC_{50} values. **StN-4**, **StN-6**, **PtP-4**, **StP-4** and **StP-10** significantly reduced ATP production (Fig 1A) after just one hour of incubation, whereas all of the compounds significantly decreased ATP production after 72 h (Fig 1B). Compound **StP-10** was the most potent one as it significantly reduced ATP production at both one and 72 hours at a concentration that was 10 times lower than that of **PtP-4** at 1 and 72 h, whereas compound **StP-4** affected ATP production only at a concentration that it was 2.5 times greater than its IC_{50}. We also measured mitochondrial membrane potential using the tetramethylrhodamine methyl ester (TMRM), a voltage sensitive dye that accumulates inside intact mitochondria, and found that one hour's treatment with the compounds had no effect, but 72 hours' treatment greatly reduced it (not shown).

Table 2. Pharmacological and biological characterization of the phosphonium compounds

Cpd	Affinity[a] α7 receptors K_i, nM (CI)	Viability[b] IC_{50}, μM U87MG 72h	Viability[b] IC_{50}, μM A549 72h	% ROS[c] production over 0.05 mM Antimycin A
PtP-4 RDM-4'BTPI	**1826** (830-4017)	**0.86**	**0.26**	**16.3**
StP-3	**984** (276-3600)	**1.4**	**1.8**	**21**
StP-4	**1638** (617-4342)	**0.64**	**0.42**	**1.5**
StP-5	**2800** (500-4280)	**0.67**	**0.32**	**20**
StP-6	**559** (31-9900)	**0.38**	**0.15**	**27.3**
StP-7	**617** (102-3700)	**0.36**	**0.12**	**39.5**
StP-8	**909** (477-1732)	**0.07**	**0.26**	**46.3**
StP-9	**1288** (614-2699)	**0.09**	**0.11**	**56.3**
StP-10	**1930** (587-6336)	**0.06**	**0.10**	**58.2**

[a] See note (a) Table 1. [b] See note (c) Table 1. [c] The FACS experiments were performed using the fluorescence indicator, a costant concentration of 500 nM of each compound and taking the ROS production induced by 50 μM antimycin as 100%.

ROS production

The quaternary onium group should target the molecules to the mitochondrial matrix, which is held at a negative relative voltage, where their pro-oxidant effect is demonstrated by increased ROS production. We therefore verified the effects of 1 h exposure to the phosphonium and ammonium compounds on the ROS production of U87MG cells as monitored by FACS experiments. Treatment

with the ammonium compounds did not induce the production of mitochondrial ROS, whereas the phosphoniums **PtP-4**, **StP-4** and **StP-10** increased ROS production in a dose- dependent manner and with an increasing potency (**StP-10** > **PtP-4** > **StP-4**) (Fig 1C).

We also tested whether there was a correlation between the length of the linker and the ability of the phosphonium compounds to produce ROS. The FACS experiments were performed using the fluorescence indicator and a costant compound concentration of 500 nM, taking the ROS production induced by 50 μM antimycin (the positive control) as 100%. As shown in Table 2, increasing the length of the linker increases the capability of phosphonium compounds to produce mitochondrial ROS.

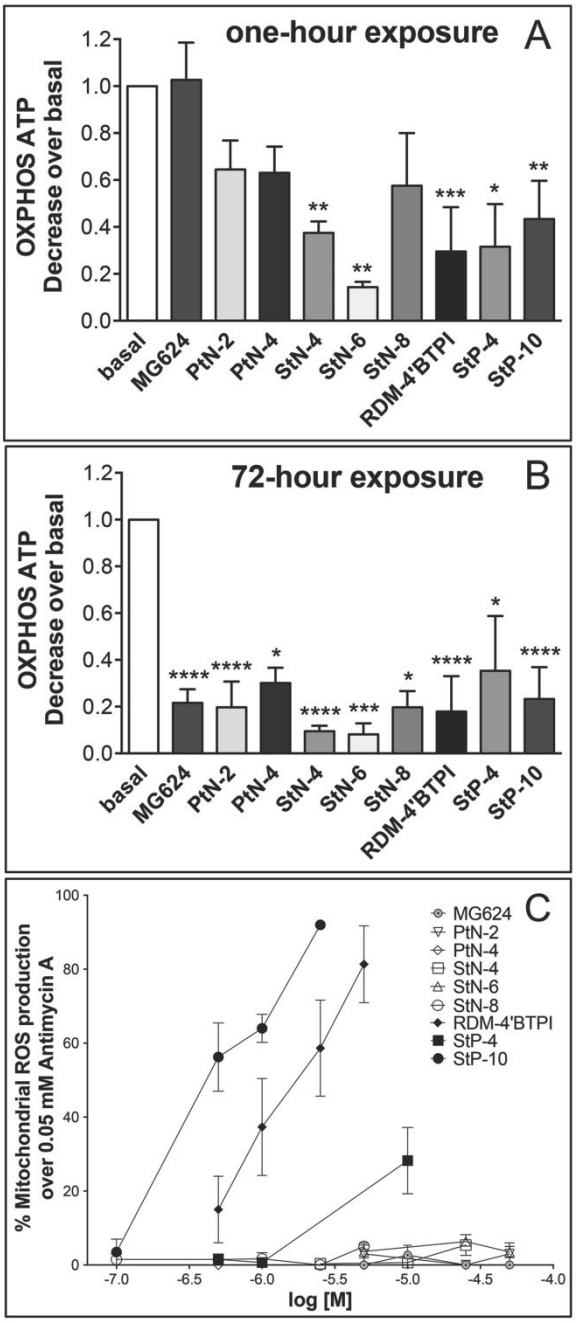

Figure 1. Effects of onium compounds on the mitochondrial ATP and ROS production in U87MG cells.

The figure shows the decrease in the level of mitocondrial ATP after one (Fig 1A) or 72 hours (Fig 1B) incubation of U87MG cells with the indicated compounds. The data shown were obtained using the concentrations of the ammonium compounds **MG624** (**StN-2**), **PtN-2**, **PtN-4 , StN-4, StN-6** and **StN-8** of respectively 4, 4, 0.5, 2, 4 and 0.25 μM and concentrations of the phosphonium compounds **RDM-4'BTPI** (**PtP-4**), **StP-4** and **StP-10** of respectively 1, 2 and 0.1 μM. For almost all cases, these concentrations correspond to the IC_{50} concentrations determined in the viability assays of U87MG cells. The data from at least five separate experiments are expressed by setting the basal level of control cells as 1 and were analysed by means of one way ANOVA followed by Dunn's *post hoc* test *P<0.05, ** P<0.01, *** P<0.001, **** P<0.0001 versus basal control. (Fig. 1 C) Relative ROS production at increasing compound concentrations. Data are expressed by setting the ROS production of the positive control 50 μM antimycin A as 100%.

HepG2 cells permeation

The ability of **StN-2** to permeate the HepG2 cells was investigated exploiting the natural behavior of **StN-2** to emit fluorescence at 350 nm after excitation at 260 nm using a fluorescent plate reader. Briefly, HepG2 cells were treated with 1.0, 10.0, 50.0, and 100.0 μM **StN-2** or vehicle (DMSO, blank samples) for 6 and 24 h, respectively. Fluorescence signals emitted at 350 nm of each compound at intracellular level have been normalized for the total amount of cells (fluorescence emission of the nuclei after their staining with DAPI) at 620 nm obtaining, therefore, the Relative Fluorescence Unit (RFU) 350/620 nm after 6 and 24 h of incubation. The RFU 350/620 nm of the blank samples, which represents the cellular background, was subtracted from each normalized fluorescence signal (RFU 350/620 nm). Our findings clearly indicated that **StN-2** is taken up by HepG2 cells with a concentration and time response trend. In particular, **StN-2** is able to permeate the human hepatic cells by 4.75, 6.82, 7.67, and 9.43 RFU at 1.0, 10.0, 50.0, and 100.0 μM, respectively after 6h. After 24 h, the fluorescence signal deriving from the intracellular level reaches 5.42, 7.18, 9.13, and 14.35 RFU, after the treatment with the compound at 1.0, 10.0, 50.0, and 100.0 μM, respectively (Figure 2).

Cells treated with 100 μM **StN-2** for 24 h were lysed and the cell lysates were analyzed by mass spectrometry. The MS/MS fragmentation pattern and the observed product ions are completely assigned to the product ions generated during the fragmentation. In the MS/MS spectrum the base peak at *m/z* 222.9 corresponds to the loss of the styrene moiety.

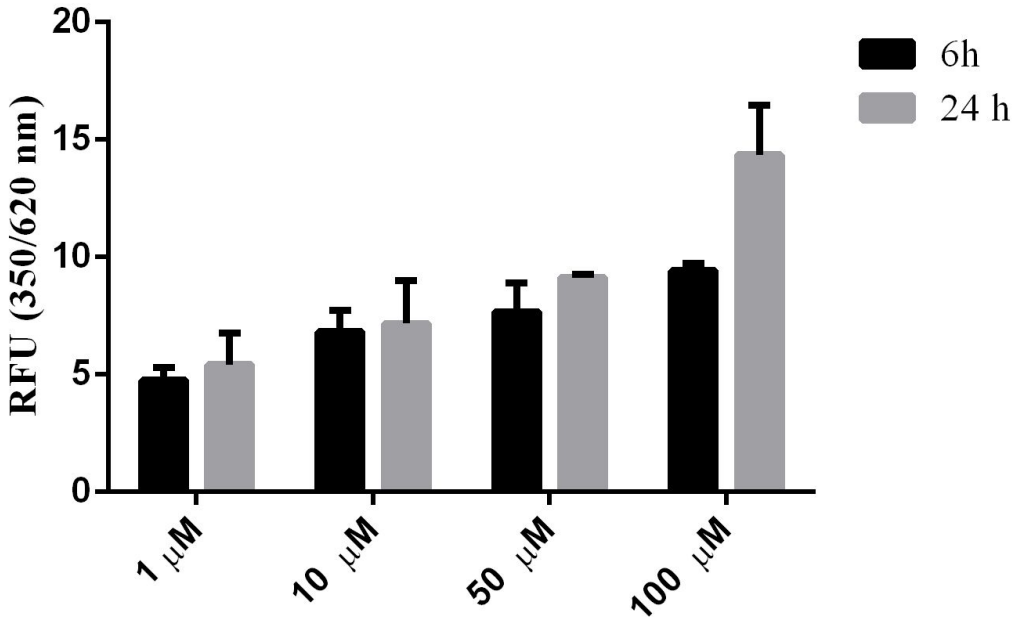

Figure 2. Fluorescence signals (bars normalized using the DAPI staining of the nuclei) of HepG2 internalized **StN-2** after 6h (black bars) and 24 h (grey bars) at different concentrations. **StN-2** naturally emits fluorescence at 350 nm after excitation at 260 nm.

We investigated the ability to permeate the HepG2 also of compounds **StN-4**, **StN-8** and **StP-8** at 1 μM concentration, after ascertaining that their fluorescence properties (emission at 350 nM upon irradiation at 260 nM) were just like those of **StN-2**. Figure 3 shows the intracellular fluorescence signals reached after 1, 6 and 24 hours treatment with the three compounds in comparison with **StN-2**. All the four compounds are able to permeate, the two longest ones, having eight-carbon linker and phosphonium or ammonium head, a little more rapidly. Overall, these experiments suggest that cell permeation should be prejudiced neither by polymethylene linker length or onium head nature and thus allowed to all our compounds.

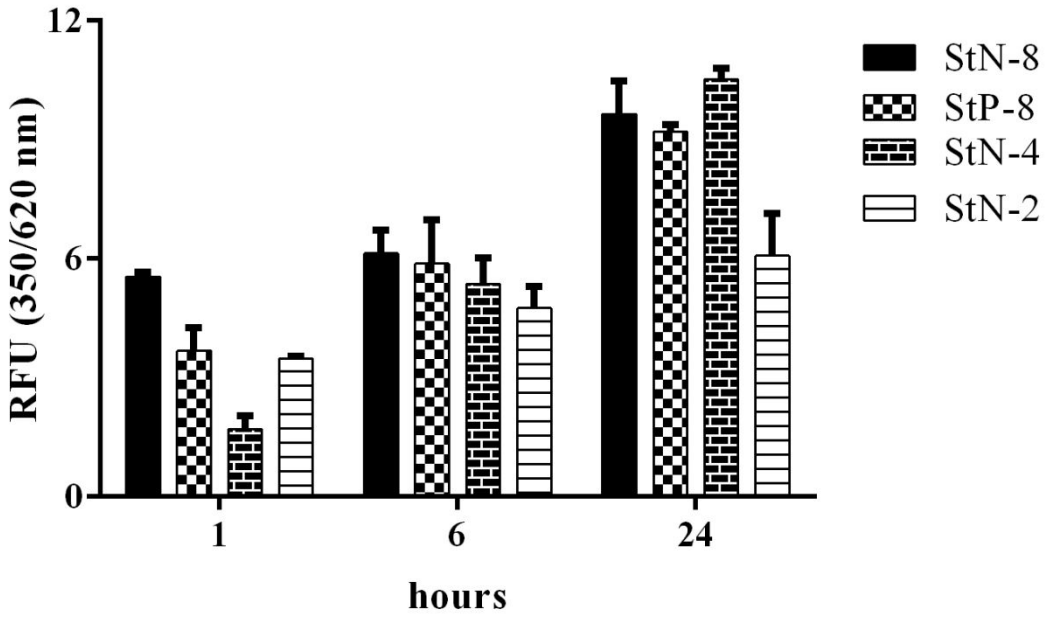

Figure 3. Fluorescence signals (bars normalized using the DAPI staining of the nuclei) of HepG2 internalized **StN-2**, **StN-4**, **StN-8** and **StP-8** after 1 h, 6 h and 24 h at 1 μM concentration.

DISCUSSION

The hybridisation planning. The two pillars of our investigation were RDM-4'BTPI (**PtP-4**) and MG624 (**StN-2**): the former, the mitochondriotropic triphenylphosphoniumbutyl ether of pterostilbene (3',5'-dimethoxy-4-stilbenol), owes its antiproliferative activity to its known cytotoxic pro-oxidant action[7]; the latter, the triethylammoniumethyl ether of 4-stilbenol, selectively antagonises ACh at α7- and α9-nAChR and, as recently found, has an antiproliferative activity, that is related to its interaction with α7- and α9-nAChRs.13 The two molecules were hybridised with the idea that recombining their similar constituents (onium head, alkyl linker and stilbene scaffold) may not only clarify the contribution of the three substructures to the various components of the antiproliferative activity, but also lead to a sort of hybridisation of the biological profiles of RDM-4'BTPI and MG624 by creating synergies between different mechanisms of action.

Nicotinic binding and nicotinic antagonist affinity of the ammonium hybrids. The synthesis of the three structural hybrids with triethylammonium head, **StN-4**, **PtN-2** and **PtN-4**, was not problematic. We could prepare the **StN-2** analogue with a four-carbon linker, **StN-4**, and the two pterostilbene analogues **PtN-2** and **PtN-4** with respectively two- and four-carbon linkers. As single modifications, the linker elongation (compound **StN-4**) and the 3',5'-dimethoxy substitution (compound **PtN-2**) only slightly diminished the α7 nicotinic affinity of **StN-2** (0.104 μM K_i), but, together, they led to a greater decrease (compound **PtN-4.** 0.3 μM K_i). Therefore, further linker elongation to six and eight carbons was accomplished in the **StN** series rather than in the **PtN** series. **StN-6** showed a decreased α7 nicotinic affinity (0.465 μM K_i), but its eight-carbon analogue **StN-8** had an α7 affinity (0.164 μM K_i) similar to that of **StN-2**. Like **StN-2**, all the five new ammonium derivatives had modest micromolar α4β2 affinity. On the basis of these findings, we tested functionally their ability to antagonise the ACh activation of the α7 and the α9α10 nicotinic subtypes heterologously expressed in oocytes. We found that the pterostilbene analogue of **StN-2**, namely **PtN-2**, was as potent as **StN-2** (IC_{50} 47 *vs* 41 nM at the α7 subtype and IC_{50} 17 vs 10 nM at the α9α10 subtype) thus indicating that the 3',5'-dimethoxy substitution is irrelevant in this respect. Consistently with these results, elongation to four carbons was beneficial for both of them: **StN-4** had IC_{50} 6.5 nM at α7 and IC_{50} 5 nM at α9α10, while **PtN-4** IC_{50} 24.3 nM at α7 and IC_{50} 11.9 nM at α9α10. Further elongation in the **StN** series to six and eight carbons confirmed the α9α10 sub-10 nM potency achieved by **StN-4** and, though not ameliorative, the considerable sub-100 nM potency of **StN-2** at the α7 subtype. Overall, as shown in Table 1, elongation of the ethylene linker in the ammonium compounds resulted in generally higher antagonist activities at the two nicotinic receptors with non-negligible α9α10 vs α7 selectivity in the case of **StN-8**.

Anti-adenocarcinoma activity of the phosphonium hybrids. On the other hand, of the three structural hybrids with phosphonium head, only **StP-4**, the stilbene analogue of **PtP-4** (RDM-4'BTPI), could be obtained as the phosphonium ethyloxy derivatives **PtP-2** and **StP-2** were highly

unstable. **PtP-4** has been characterised in detail as a mitocan by its inventors, who reported that it induces the necrotic death of CT-26 mouse colon tumor cells in the low-μM range and that it is respectively 5-fold and 10-100-fold more potent than its demethylated analogue and resveratrol, which has all three phenolic hydroxyls free and is therefore not mitochondriotropic[7]. Its cytotoxicity is due to the production of ROS, particularly of H_2O_2, upon accumulation in mitochondria and there is evidence that, like mitoVES, it induces the generation of ROS by interacting with respiratory chain complexes anchored in the mitochondrial inner membrane[16].

Supported by these data, we decided to test the antiproliferative activity of the two phosphonium derivatives, **PtP-4** and **StP-4**, on the A549 adenocarcinoma cell line derived from lung tumors, the same cell line as that previously used to investigate the antiproliferative properties of **StN-2**. These cells express α7 and α9 nAChRs, whose activation promotes lung carcinoma cell growth, and **StN-2** not only blocks the α7- and α9-mediated pro-proliferative effects of nicotine on A549 cells, but also has dose-dependent A549 cytotoxicity.[13] We found that both **PtP-4** and **StP-4** have sub-micromolar cytotoxicity (0.26 and 0.42 μM IC_{50}) on A549 cells that is comparable with their low-μM cytotoxicity for CT-26 mouse colon tumor cells.[7] Importantly, these data indicate that replacing 3',5'-dimethoxystilbene with stilbene does not negatively affect antitumor activity and allowed us to undertake a systematic comparison among our six triethylammonium and triphenylphosphonium hybrids.

Comparison of the antitumoral activity of ammonium and phosphonium hybrids. In addition to the A549 human lung carcinoma line, we also used the human SH-SY5Y neuroblastoma and U87MG glioblastoma cell lines. It has been proved that glioblastoma cells express both α7 and α9 mRNAs,[17] while neuroblastoma cells express α7 mRNA and protein.[18] As shown in Table 1, the four triethylammonium derivatives **StN-2**, **PtN-2**, **PtN-4** and **StN-4** had less A549 cytotoxicity than the two triphenylphosphonium compounds, **PtP-4** and **StP-4**; their IC_{50} values are in the 3-12 μM range, whereas those of **PtP-4** and **StP-4** are in the 0.2-0.5 μM range. In particular, the antiproliferative

activity of **StN-2** (4.4 μM IC_{50}) confirmed the extent of the previously observed decrease in A549 cell proliferation.[13] Furthermore, compounds **StN-4** and **PtN-4**, with four-carbon O-N^+ linker, showed slightly greater A549 cytotoxicity (respectively 3.5 and 3.3 μM IC_{50}). Viability assays of the neuroblastoma and glioblastoma cells followed similar trends but with some noteworthy divergences. When tested on neuroblastoma cells the two phosphonium compounds **PtP-4** and **StP-4** were more potent (respectively 0.55 and 3.0 μM IC_{50}) than the elongated ammonium compounds **PtN-4** and **StN-4** (11 and 31 μM IC_{50}), in turn much more potent than their shorter analogues **PtN-2** and **StN-2**. On the other hand, compounds **PtN-4** and **StN-4** were as potent as the two phosphoniums against glioblastoma, thus showing pronounced glioblastoma vs neuroblastoma selectivity, and, notably, they were much less toxic than the two phosphoniums towards normal glial cells.

Mechanisms of action. After investigating their antiproliferative activity on various tumor cells, we investigated whether the six hybrids mechanisms of action underlying their antitumor activity were similar by considering two intracellular parameters: the increase in mitochondrial ROS generation and the decrease in ATP production in U87MG cells. We first ascertained that the triethylammoniumalkyl derivatives can permeate cell membranes, as reported for RDM-4'BTPI and other molecules linked to triphenylphosphonium through an aliphatic carbon chain. Initially, we considered **StN-2** and **StN-4**. The ability to permeate the HepG2 cells was investigated using two different approaches. The former permitted to detect **StN-2** and **StN-4** directly in intact cells exploiting their natural ability to emit fluorescence at 350 nm after excitation at 260 nm, whereas the latter, applied only to **StN-2**, was based on the detection of **StN-2** in the cell lysates by LC-MS/MS. Both approaches suggest that the two ammoniums are bioavailable at intracellular levels. In particular, already after 1 h, HepG2 cells were able to uptake them from the extracellular environment with a concentration-response trend, which was highly improved after 24 h of treatment (Figure 2 and 3). In agreement with this result MS analysis unequivocally confirmed the presence of **StN-2** in the HepG2 cell lysates after 24 h treatment. As shown in Figure 1C, mitochondrial ROS production

was induced in U87MG glioblastoma cells by **PtP-4** (RDM-4'BTPI) and **StP-4**, but not by the four ammonium derivatives, **StN-2**, **StN-4**, **PtN-2** and **PtN-4**. Phosphonium **StP-4** was about 10-fold less potent than RDM-4'BTPI, whose response in glioblastoma cells at a concentration of 1μM, after one hour incubation, was almost identical to that reported in Jurkat cells at the same concentration and after the same incubation time.[7]

The second intracellular parameter we examined was the decrease in ATP production, which is indicative of dysregulated mitochondrial function and antitumor activity.[19] Tumor cells have to up-regulate their inefficient glycolytic ATP production in order to satisfy their energy requirements and preventing mitochondrial ATP production has a highly toxic and antiproliferative effect. There was a reduction in the ATP production in glioblastoma cells, as early as one hour after the administration of **PtP-4**, **StP-4** and **StN-4**, whereas ATP was significantly reduced only after 72 hours in the case of the other three ammonium derivatives, **StN-2**, **PtN-2** and **PtN-4**.

In order to complete the picture symmetrically, we had to establish whether the two phosphonium hybrids, **PtP-4** and **StP-4**, have α7 nicotinic affinity and, if so, whether they have antagonist activity at α7 nAChRs. The data shown in Table1 indicate that **PtP-4** and **StP-4** have very modest supramicromolar binding affinity for α7 nAChRs and that the IC_{50} of **PtP-4** for Ach activated α7 and α9α10 nAChRs is greater than 10 μM.

Overall, the results of these experiments indicate that the mechanism of action underlying the antitumor activity of the triphenylphosphonium derivatives is the profound impairment of mitochondrial functions, as revealed by the immediate and conspicuous increase in ROS production and decrease in ATP production and by their quite indistinct cytotoxicity. On the other hand, the antitumor activity of the triethylammonium derivatives seems to be mainly connected to their interactions with α7 and α9α10 nAChRs. However it cannot be excluded that, after entering cells, the triethylammonium derivatives, interfere with mitochondria function albeit less potently than the phosphonium analogues possibly due to a delayed membrane crossing and a lower level of

mitochondriotropism. This may be why, with the exception of **StN-4**, our triethylammonium derivatives decreased ATP production, only after 72 hours, and induced no immediate increase in ROS production.

Multi-carbon linker elongation in ammonium and phosphonium compounds. As stated in the introduction, alkylene elongation was expected to be the most promising modification of **StN-2** resulting from its hybridisation with the **PtP-4** substructures, and **StN-4** proved to be a more potent α7 and α9α10 nAChR antagonist than **StN-2** and **PtN-2** and, together with **PtN-4**, had greater antitumor activity, particularly against glioblastoma cells. Such a trend was substantially confirmed by the further elongation of the linker to six and eight methylenes. Compared with **StN-4**, compound **StN-8** showed a 16-fold more potent anti-glioblastoma activity, characterized by higher selectivity over the other tumor and non-tumor cells. Interestingly, such a profile was associated with maintaining the highly potent α9α10 nAChR antagonism reached by **StN-4** and improvement of ATP production impairment.

With regard to linker length in the phosphoniums, shortening the four-carbon bridge of **PtP-4** by two carbons was not only hampered by the high chemical instability of the triphenylphosphoniumethyloxy residue, but was also discouraged by the finding that **PtP-4** and **StP-4** have modest nicotinic affinity and no antinicotinic properties, probably due to the unsuitable triphenyl substitution at P^+ regardless of the length of the alkylene linker. Furthermore, SAR studies have recently been made on the mitochondrially targeted derivative of vitamin E (VE) analogus α-tocopheryl succinate, MitoVES (or $MitoVE_{11}S$), which has an eleven-carbon linker between its triphenylphosphonium head and chromane nucleus.[14] $MitoVE_{11}S$ inhibits mitochondrial respiratory complex II (CII) leading to ROS generation and cell death induction with IC_{50} values for apoptosis in various malignant cell lines mainly ranging between 0.5 and 3 μM. [20] A similar mechanism of action, preferentially involving CI and CIII, has been invoked also in support to **PtP-4** proapoptotic activity, [16] for which we determined slightly higher cytotoxicity values (0.86, 0.55 and 0.26 μM IC_{50} on U87MG, SH-SY5Y and A549 cell lines respectively). These SAR studies on $MitoVE_{11}S$ have

highlighted that a key role is played by the suitable length of the linker between the targeting group (P^+Ph_3) and the group responsible for the interaction with the binding site of the mitochondrial complex. [14] Short-linker analogs, such as $MitoVE_9S$, $MitoVE_7S$ and $MitoVE_5S$, show decreasing effects with the number of carbons of the linker suggesting that their bioactive group cannot reach the binding site.

On the basis of these observations, we wondered whether increasing the four-carbon distance between the stilbenoxy group and the triphenylphosphonium head of **StP-4** would lead to a parallel increase in activity. The answer was yes. Though with some slight incongruities, anti-glioblastoma and anti-adenocarcinoma activities gradually increase with the number of carbons (compounds **StP-5→StP-9**). Compound **StP-10**, whose linker is ten-carbon long, was 10-fold (vs U87MG) and four-fold (vs A549) more potent than compound **StP-4** and also more potent than its long-bridged analogue $MitoVE_{11}S$. Consistently, compound **StP-3**, which has a shortened three-carbon linker, was 2-fold less cytotoxic for glioblastoma cells than **StP-4** and 4-fold less cytotoxic for adenocarcinoma cells. Linker elongation gradually increased also ROS generation: compound **StP-10** was almost four-fold more potent than **PtP-4** and 39-fold more potent than **StP-4**. Furthermore, the decrease in ATP production was observable as early as one hour after the administration of **StP-10**.

In view of these findings, the greater antitumor activity of the elongated ammonium derivatives in comparison with **StN-2** and **PtN-2** may also be due to the wider spacing between the onium head and stilbene portion, a modification beneficial for the interaction at mitochondrial level.

Fluorescence experiments with HepG2 cells demonstrated that elongated ammonium and phosphonium compunds (**StN-8** and **StP-8**) are able to rapidly permeate cell membrane.

CONCLUSIONS

Adenocarcinoma, neuroblastoma and glioblastoma cell lines express α7- and, excepting for neuroblastoma, α9-containing nAChRs, whose activation has been proved to increase cell proliferation. A specific antagonist of these receptors, **StN-2** (MG624), reduces the viability of such tumor cells in a dose-dependent manner. Its structure, a quaternary ammonium head linked through an alkylenoxy chain to the stilbene para position, resembles that of the known mitocan RDM-4'BTPI (**PtP-4**), the triphenylphosphoniumbutyl ether of pterostilbene, which we found to be cytotoxic for the same tumors impairing mitochondrial functions. The hybridisation of these two lead compounds by recombining their three structural elements (onium head, alkyleneoxy linker and stilbene or 3',5'-dimethoxystilbene scaffold) and lengthening the polyalkylene chain proved to be a profitable design approach, as summarized in Table 3, which lists the magnitude of the action mechanisms and of the cytotoxicities.

Table 3. Mechanisms of action of compounds reported in Table 1

CPD	nAChR ANTAGONISM	ACTION ON MITOCHONDRIA	MITOCHONDRIAL ROS PRODUCTION ($O_2^{\cdot-}$)	OXPHOS ATP DECREASE		CELL VIABILITY / PROLIFERATION DECREASE AT
				1h	72h	
StN-2 (MG624)	++	INDIRECT (72h)	-	-	↓	[μM]
PtN-2	++	INDIRECT (72h)	-	-	↓	[μM]
PtN-4	++	INDIRECT (72h)	-	-	↓↓	**[nM]**
StN-4	++	**DIRECT (1h)**	-	↓	↓	[μM]
StN-6	++	**DIRECT (1h)**	-	↓	↓	[μM]
StN-8	++	INDIRECT (72h)	-	-	↓↓	**[nM]**
PtP-4 (RDM-4'BTPI)	-	**DIRECT (1h)**	↑	↓	↓	[μM]
StP-4	-	**DIRECT (1h)**	↑	↓	↓	**[nM]**
StP-10	-	**DIRECT (1h)**	↑↑	↓↓	↓↓	**[nM]**

The two ammonium hybrids **StN-4** and **PtN-4** with linker elongated to butylene were more toxic against cancer cells, particularly glioblastoma cells, and their potency was similar to the submicromolar potency of **PtP-4**, but they were more selective and less toxic against non-tumor cells than **PtP-4**. Notably, the enhanced anti-glioblastoma activity of compound **StN-4** coincided with greater antagonism against α7 and α9 nAChRs and **StN-4** was the only ammonium hybrid capable of reducing mitochondrial ATP production after 1h. Such a positive trend was confirmed by further elongation to six and eight carbons (**StN-6** and **StN-8**).

Hybridisation of the phosphonium derivatives was limited to replacing pterostilbene with stilbene for feasibility reasons. This modification of **PtP-4** (compound **StP-4**) did not prejudice its ability to impair mitochondrial function, but it did not confer, as expectable, those antinicotinic properties of which, as we demonstrated, **PtP4** is devoid. Nevertheless, the approach was effective in suggesting that further elongation of the linker would also benefit the pro-oxidant cytotoxic activity of triphenylphosphonium derivatives. The analogue of **StP-4** with a ten-carbon linker (compound **StP-10**) was a much more potent mitocan than both **PtP-4** and **StP-4**, which have butylene linkers.

In conclusion, we developed more potent antitumor triphenylphosphonium analogues of RDM-4'BTPI, and we have also demonstrated that the less lipophilic triethylammoniumalkyloxystilbenes, hitherto considered as acting at membrane α7 and α9 nAChRs, cross membranes and interfere with mitochondrial functionality. Interestingly, we found that enhancement of such a capacity, associated with more potent α7 and α9 antagonism, as in ammonium compounds **StN-4**, **StN-6** and, above all, **StN-8**, improves the moderate antitumor activity of the quaternary ammonium **StN-2** without impairing its selectivity.

EXPERIMENTAL SECTION

Chemistry. All chemicals and solvents were used as received from commercial sources or prepared as described in the literature. Flash chromatography purifications were performed using KP-Sil 32-63 μm 60 Å cartridges. TLC analyses were carried out on alumina sheets precoated with silica gel 60 F254 and visualized with UV light; Rf values are given for guidance. ^{1}H and ^{13}C NMR spectra were recorded at 300 and 75 MHz using an FT-NMR spectrometer. Chemical shifts are reported in ppm relative to residual solvent ($CHCl_3$, MeOH or DMSO) as internal standard. Melting points were determined by Buchi Melting Point B-540 apparatus. Elemental analyses (CHN) are within ± 0.40% of theoretical values. The results of elemental analyses indicated that the purity of all tested compounds was higher than 95%. In each described preparation, the moles of reagents are given for one mmole of substrate.

METHOD A: general procedure for the preparation of 1a and 1c.

The intermediates **1a** and **1c** were synthesized according to a modified literature procedure.[21] K_2CO_3 (1.1 mmol) was added to a solution of resveratrol (1 mmol) in 1.2 ml of anhydrous DMF. After stirring for 20 minutes, the appropriate bromo-chloro-alkane (1.5 mmol, 1-bromo-2-cloroethane for **1a** and 1-bromo-4-chlorobutane for **1c**) was added dropwise and the reaction mixture was stirred overnight at 60 °C. After HCl/AcOEt extraction, the organic phase was dried over $NaSO_4$, filtered and evaporated under vacuum. The crude residue was then purified by flash column chromatography, affording the desired intermediates as brownish solids.

METHOD B: general procedure for the preparation of 4b-i

The intermediates **4b-i** were synthesized according to a modified literature procedure.[22] A solution of *trans*-4-hydroxy-stilbene (1 mmol) in DMSO (1.4 ml) was added to a stirred suspension of 85 mg of finely ground NaOH (2.1 mmol) in DMSO (5.6 ml). The mixture was stirred at room temperature for 30 minutes and then the appropriate dibromoalkane (2 mmol) was added dropwise. After 3 hours, the reaction mixture was filtered and 1M aqueous solution of HCl was added dropwise to the filtrate to reach pH 3. The crude product was precipitated by slowly adding cold water. The precipitate was

isolated by filtration, dried under vacuum and recrystallized from ethanol affording the desired intermediates as white solids. In the only case of the bromopropyl ether **4b**, purification was accomplished by chromatography.

METHOD C: general procedure for the preparation of 2a and 2c

The intermediates **2a** and **2c** were prepared according to a modified literature procedure.[21] Cs_2CO_3 (2.2 mmol) was added to a stirred solution of the appropriate precursor (1 mmol of **1a** and **1c** respectively) in anhydrous DMF (1.5 ml). The resultant mixture was stirred for 20 minutes. Afterward, MeI (2.2 mmol) was added dropwise and the reaction mixture was stirred overnight at room temperature. After HCl/EtOAc extraction, the organic phase was dried over $NaSO_4$, filtered and concentrated under vacuum. The crude residue was then purified by flash column chromatography, affording the desired intermediates as solids.

METHOD D: general procedure for the preparation of 3a, 3c and 5b-i

The intermediates **3a**, **3c** and **5b-i** were obtained by dissolving **2a**, **2c** and **4b-i** (1 mmol), respectively, in a saturated solution of NaI in acetone (10 ml), which was then refluxed overnight. After concentrating under vacuum, the residue was diluted with diethyl ether and subsequently washed with 10% aqueous $Na_2S_2O_5$ and then with brine. The organic phase was dried over Na_2SO_4, filtered, and the solvent was evaporated under vacuum to give the desired intermediates as solids.

METHOD E: general procedure for the preparation of PtN-2, PtN-4, StN-4, StN-6, StN-8

The compounds **PtN-2**, **PtN-4**, **StN-4**, **StN-6** and **StN-8** were obtained by stirring **3a**, **3c**, **5c**, **5e** and **5g** (1 mmol), respectively, triethylamine (3 ml – 21.6 mmol) and toluene (3 ml) at reflux temperature for 5 hours. Upon concentration under vacuum, the residue was diluted with diethyl ether and the obtained suspension was filtered, affording the desired product as a solid.

METHOD F: general procedure for the preparation of compounds StP-3-StP-10

The compounds **StP-3-StP-10** were obtained by heating a solid mixture of PPh_3 (20 mmol) and the respective iodinated precursor **5b-i** (1 mmol) to 100 °C so as to obtain a solution of the starting material in molten PPh_3. The reaction mixture was slowly stirred at 100 °C for 3 hours and then cooled to room temperature without stirring any further. The re-solidified mixture was dissolved in the smallest possible volume of dichloromethane and diethyl ether was added dropwise under vigorous stirring. Afterwards, the solid precipitate was isolated by filtration affording the desired products.

(*E*)-3',5'-Dihydroxy-4-(2-chloroethyloxy)stilbene (1a)

Obtained from resveratrol according to METHOD A, as a brown solid in 32% yield after purification through silica gel chromatography (gradient dichloromethane/ethyl acetate from 9:1 to 8:2). Rf (dichloromethane/ethyl acetate 9:1) = 0.22. M.p.= 161 °C. ^{1}H NMR (300 MHz, DMSO) δ 9.20 – 9.13 (s, 2H, exchange with water), 7.49 (d, *J* = 8.8 Hz, 2H), 7.02 – 6.81 (m, 4H), 6.38 (d, *J* = 2.2 Hz, 2H), 6.10 (t, *J* = 2.2 Hz, 1H), 4.29 – 4.20 (m, 2H), 3.97 – 3.87 (m, 2H).

(*E*)-3',5'-Dihydroxy-4-(4-chlorobutyloxy)stilbene (1c)

Obtained from resveratrol according to METHOD A, as a light brown solid in 30% yield after purification through silica gel chromatography (gradient from dichloromethane to dichloromethane/methanol 9:1). Rf (dichloromethane/methanol 9:1) = 0.54. M.p.= 148 °C. ^{1}H NMR (300 MHz, DMSO) δ 9.18 (s, 2H, exchange with water), 7.48 (d, *J* = 8.7 Hz, 2H), 6.91 (m, 4H), 6.38 (d, *J* = 2.0 Hz, 2H), 6.10 (t, *J* = 2.0 Hz, 1H), 4.00 (t, *J* = 5.9 Hz, 2H), 3.70 (t, *J* = 5.9 Hz, 2H), 1.97 – 1.70 (m, 4H).

(*E*)-3',5'-Dimethoxy-4-(2-chloroethyloxy)stilbene (2a)

Obtained from **1a** according to METHOD C as a salmon solid in 90% yield after purification by silica gel chromatography (cyclohexane/ethyl acetate 9:1). Rf (cyclohexane/ethyl acetate 9:1) = 0.37. M.p.= 86-88 °C. ^{1}H NMR (300 MHz, $CDCl_3$) δ 7.44 (d, *J* = 8.7 Hz, 2H), 7.03 (d, *J* = 16.3 Hz, 1H), 6.96 –

6.85 (m, 3H), 6.64 (d, *J* = 2.2 Hz, 2H), 6.37 (t, *J* = 2.2 Hz, 1H), 4.25 (t, *J* = 5.9 Hz, 2H), 3.85 – 3.79 (m, 8H).

(*E*)-3',5'-Dimethoxy-4-(4-chlorobutyloxy)stilbene (2c)

Obtained from **1c** according to METHOD C as a pale yellow solid in 63% yield after purification by silica gel chromatography (cyclohexane/ethyl acetate 95:5). Rf (cyclohexane/ethyl acetate 95:5) = 0.22. M.p.= 77 °C. ^{1}H NMR (300 MHz, $CDCl_3$) δ 7.43 (d, *J* = 8.6 Hz, 2H), 7.03 (d, *J* = 16.2 Hz, 1H), 6.95 – 6.81 (m, 3H), 6.65 (d, *J* = 1.9 Hz, 2H), 6.37 (t, *J* = 1.9 Hz, 1H), 4.03 (d, *J* = 5.8 Hz, 2H), 3.83 (s, 6H), 3.63 (t, *J* = 5.8 Hz, 2H), 1.97 (m, 4H).

(*E*)-3',5'-Dimethoxy-4-(2-iodoethyloxy)stilbene (3a)

Obtained from **2a** according to METHOD D. Yield: 97%. M.p.: 82-84 °C. Rf (cyclohexane/ethyl acetate 9:1) = 0.43. ^{1}H NMR (300 MHz, $CDCl_3$) δ 7.44 (d, *J* = 8.8 Hz, 2H), 7.03 (d, *J* = 16.3 Hz, 1H), 6.91 (m 3H), 6.64 (d, *J* = 2.2 Hz, 2H), 6.38 (t, *J* = 2.2 Hz, 1H), 4.27 (t, *J* = 6.9 Hz, 2H), 3.82 (s, 6H), 3.45 – 3.39 (t, *J* = 6.9 Hz, 2H).

(*E*)-3',5'-Dimethoxy-4-(4-iodobutyloxy)stilbene (3c)

Obtained from **2c** according to METHOD D. Yield: 96%. M.p.: 87°C. Rf (cyclohexane/ethyl acetate 9:1) = 0.36. ^{1}H NMR (300 MHz, $CDCl_3$) δ 7.43 (d, *J* = 8.7 Hz, 2H), 7.03 (d, *J* = 16.3 Hz, 1H), 6.96 – 6.76 (m, 3H), 6.65 (d, *J* = 2.2 Hz, 2H), 6.38 (t, *J* = 2.2 Hz, 1H), 4.01 (t, *J* = 6.0 Hz, 2H), 3.83 (s, 6H), 3.27 (t, *J* = 6.8 Hz, 2H), 2.14 – 1.85 (m, 4H).

(*E*)-4-(3-Bromopropyloxy)stilbene (4b)

Obtained from 4-stilbenol synthesized according to METHOD B by reaction with 1,3-dibromopropane. The crude product was purified by silica gel chromatography (gradient from hexane to hexane/acetonitrile 9:1). Yield: 52%. M.p.: 109 °C. Rf (hexane/acetonitrile 9:1) = 0.24. ^{1}H NMR (300 MHz, $CDCl_3$) δ 7.54 – 7.41 (m, 4H), 7.35 (t, *J* = 6.7 Hz, 2H), 7.26 – 7.19 (m, 1H), 7.08 (d, *J* = 15.5 Hz, 1H), 7.03 – 6.87 (m, 3H), 4.14 (t, *J* = 6.4 Hz, 2H), 3.62 (t, *J* = 7.0 Hz, 2H), 2.34 (m, 2H).

(*E*)-4-(4-Bromobutyloxy)stilbene (4c)

Obtained from 4-stilbenol according to METHOD B by reaction with 1,4-dibromobutane. Yield: 37%. M.p.: 115 °C. Rf (cyclohexane/ethyl acetate 9:1) = 0.61. ^{1}H NMR (300 MHz, $CDCl_3$) δ 7.50 – 7.43 (m, 4H), 7.34 (t, *J* = 7.7 Hz, 2H), 7.23 (m, 1H), 7.06 (d, *J* = 16.3 Hz, 1H), 6.97 (d, *J* = 16.3 Hz, 1H), 6.88 (d, *J* = 8.7 Hz, 2H), 4.02 (t, *J* = 5.9 Hz, 2H), 3.50 (t, *J* = 6.5 Hz, 2H), 2.16 – 2.02 (m, 2H), 2.00 – 1.93 (m, 2H).

(*E*)-4-(5-Bromopentyloxy)stilbene (4d)

Obtained from 4-stilbenol according to METHOD B by reaction with 1,5-dibromopentane. Yield: 28%. M.p.: 98°C. Rf (cyclohexane/ethyl acetate 9:1) = 0.62. ^{1}H NMR (300 MHz, $CDCl_3$) δ 7.46 (m, 4H), 7.34 (t, *J* = 7.6 Hz, 2H), 7.22 (m, 1H), 7.07 (d, *J* = 16.4 Hz, 1H), 6.97 (d, *J* = 16.4 Hz, 1H), 6.88 (d, *J* = 8.7 Hz, 2H), 3.99 (t, *J* = 6.3 Hz, 2H), 3.45 (t, *J* = 6.7 Hz, 2H), 2.02 – 1.89 (m, 2H), 1.89 – 1.77 (m, 2H), 1.65 (m, 2H).

(*E*)-4-(6-Bromohexyloxy)stilbene (4e)

Obtained from 4-stilbenol according to METHOD B by reaction with 1,6-dibromohexane. Yield: 40%. M.p.: 111 °C. Rf (cyclohexane/ethyl acetate 9:1) = 0.62. ^{1}H NMR (300 MHz, $CDCl_3$) δ 7.46 (m, 4H), 7.34 (t, *J* = 7.6 Hz, 2H), 7.25 – 7.18 (m, 1H), 7.06 (d, *J* = 16.4 Hz, 1H), 6.96 (d, *J* = 16.4 Hz, 1H), 6.88 (d, *J* = 7.9 Hz, 2H), 3.98 (t, *J* = 6.4 Hz, 2H), 3.42 (t, *J* = 6.7 Hz, 2H), 1.96 – 1.73 (m, 4H), 1.55 – 1.44 (m, 4H).

(*E*)-4-(7-Bromoheptyloxy)stilbene (4f)

Obtained from 4-stilbenol according to METHOD B by reaction with 1,7-dibromoeptane. Yield: 41%. M.p.: 111 °C. Rf (cyclohexane/ethyl acetate 9:1) = 0.62. ^{1}H NMR (300 MHz, $CDCl_3$), 7.45 (m, 4H), 7.33 (t, *J* = 7.3 Hz, 2H), 7.23 (m, 1H), 7.05 (d, *J* = 16.3 Hz, 1H), 6.95 (d, *J* = 16.3 Hz, 1H), 6.87 (d, *J* = 8.5 Hz, 2H), 3.96 (t, *J* = 6.2 Hz, 2H), 3.40 (t, *J* = 6.7 Hz, 2H), 1.95 – 1.70 (m, 4H), 1.47 (m, 6H).

(*E*)-4-(8-Bromooctyloxy)stilbene (4g)

Obtained from 4-stilbenol according to METHOD B by reaction with 1,8-dibromooctane. Yield: 45%. M.p.: 110 °C. Rf (cyclohexane/ethyl acetate 9:1) = 0.63. ^{1}H NMR (300 MHz, $CDCl_3$) δ 7.46 (m, 4H), 7.34 (t, *J* = 7.5 Hz, 2H), 7.2 (m, 1H), 7.07 (d, *J* = 16.3 Hz, 1H), 6.96 (d, *J* = 16.3 Hz, 1H), 6.88 (d, *J* = 8.6 Hz, 2H), 3.97 (t, *J* = 6.5 Hz, 2H), 3.41 (t, *J* = 6.8 Hz, 2H), 1.92 – 1.72 (m, 4H), 1.52 – 1.27 (m, 8H).

(*E*)-4-(9-Bromononyloxy)stilbene (4h)

Obtained from 4-stilbenol according to METHOD B by reaction with 1,9-dibromononane. Yield: 84%. M.p.: 111 °C. Rf (cyclohexane/ethyl acetate 9:1) = 0.63. ^{1}H NMR (300 MHz, $CDCl_3$) δ 7.46 (m, 4H), 7.34 (t, *J* = 7.5 Hz, 2H), 7.23 (m, 1H), 7.07 (d, *J* = 16.3 Hz, 1H), 6.96 (d, *J* = 16.3 Hz, 1H), 6.88 (d, *J* = 8.7 Hz, 2H), 3.97 (t, *J* = 6.5 Hz, 2H), 3.41 (t, *J* = 6.8 Hz, 2H), 1.95 – 1.68 (m, 4H), 1.49 – 1.24 (m, 10H).

(*E*)-4-(10-Bromodecyloxy)stilbene (4i)

Obtained from 4-stilbenol according to METHOD B by reaction with 1,10-dibromodecane. Yield: 37%. M.p.: 112 °C. Rf (cyclohexane/ethyl acetate 9:1) = 0.63. ^{1}H NMR (300 MHz, $CDCl_3$) δ 7.46 (m, 4H), 7.34 (t, *J* = 7.6 Hz, 2H), 7.23 (m, 1H), 7.06 (d, *J* = 16.3 Hz, 1H), 6.96 (d, *J* = 16.3 Hz, 1H), 6.89 (d, *J* = 8.7 Hz, 2H), 3.97 (t, *J* = 6.5 Hz, 2H), 3.41 (t, *J* = 6.9 Hz, 2H), 1.93 – 1.71 (m, 4H), 1.49 – 1.23 (m, 12H).

(*E*)-4-(3-Iodopropyloxy)stilbene (5b)

Obtained from **4b** according to METHOD D. Yield: 98%. M.p.: 117 °C. Rf (cyclohexane/ethyl acetate 9:1) = 0.69. ^{1}H NMR (300 MHz, CDCl3) δ 7.47 (m, 4H), 7.34 (t, *J* = 7.4 Hz, 2H), 7.23 (m, 1H), 7.07 (d, *J* = 16.2 Hz, 1H), 6.97 (d, *J* = 16.2 Hz, 1H), 6.89 (d, *J* = 8.8 Hz, 2H), 4.07 (t, *J* = 5.4 Hz, 2H), 3.38 (t, *J* = 6.2 Hz, 2H), 2.29 (m, 2H).

(*E*)-4-(4-Iodobutyloxy)stilbene (5c)

Obtained from **4c** according to METHOD D. Yield: 99%. M.p.: 124 °C. Rf (cyclohexane/ethyl acetate 9:1) = 0.66. ^{1}H NMR (300 MHz, $CDCl_3$) δ 7.47 (m, 4H), 7.34 (t, *J* = 7.6 Hz, 2H), 7.23 (m, 1H), 7.06

(d, *J* = 16.3 Hz, 1H), 6.97 (d, *J* = 16.3 Hz, 1H), 6.88 (t, *J* = 8.7 Hz, 2H), 4.01 (t, *J* = 6.0 Hz, 2H), 3.27 (t, *J* = 6.8 Hz, 2H), 2.12 – 1.98 (m, 2H), 1.98-1.83 (m, 2H).

(*E*)-4-(5-Iodopentyloxy)stilbene (5d)

Obtained from **4d** according to METHOD D. Yield: 100%. M.p.: 102°C. Rf (cyclohexane/ethyl acetate 9:1) = 0.68. ^{1}H NMR (300 MHz, $CDCl_3$) δ 7.47 (m, 4H), 7.34 (t, *J* = 7.5 Hz, 2H), 7.23 (m, 1H), 7.06 (d, *J* = 16.3 Hz, 1H), 6.96 (d, *J* = 16.3 Hz, 1H), 6.88 (d, *J* = 8.7 Hz, 2H), 3.99 (t, *J* = 6.3 Hz, 2H), 3.23 (t, *J* = 7.0 Hz, 2H), 1.99 – 1.74 (m, 4H), 1.68 – 1.56 (m, 2H).

(*E*)-4-(6-Iodohexyloxy)stilbene (5e)

Obtained from **4e** according to METHOD D. Yield: 100%. M.p.: 126 °C. Rf (cyclohexane/ethyl acetate 9:1) = 0.76. ^{1}H NMR (300 MHz, $CDCl_3$) δ 7.47 (m, 4H), 7.34 (t, *J* = 7.6 Hz, 2H), 7.23 (m, 1H), 7.06 (d, *J* = 16.3 Hz, 1H), 6.96 (d, *J* = 16.3 Hz, 1H), 6.88 (d, *J* = 8.6 Hz, 2H), 3.98 (t, *J* = 6.4 Hz, 2H), 3.20 (t, *J* = 6.7 Hz, 2H), 1.93 – 1.72 (m, 4H), 1.50 – 1.37 (m, 4H).

(*E*)-4-(7-Iodoheptyloxy)stilbene (5f)

Obtained from **4f** according to METHOD D. Yield: 100%. M.p.: 84 °C. Rf (cyclohexane/ethyl acetate 9:1) = 0.76. ^{1}H NMR (300 MHz, $CDCl_3$) δ 7.47 (m, 4H), 7.34 (t, *J* = 7.7 Hz, 2H), 7.22 (m, 1H), 7.06 (d, *J* = 16.3 Hz, 1H), 6.96 (d, *J* = 16.3 Hz, 1H), 6.88 (d, *J* = 8.6 Hz, 2H), 3.97 (t, *J* = 6.5 Hz, 2H), 3.19 (t, *J* = 6.0, *J* = 4.2 Hz, 2H), 1.89 – 1.72 (m, 4H), 1.44 (m, 6H).

(*E*)-4-(8-Iodooctyloxy)stilbene (5g)

Obtained from **4g** according to METHOD D. Yield: 99%. M.p.: 120 °C. Rf (cyclohexane/ethyl acetate 9:1) = 0.74. ^{1}H NMR (300 MHz, $CDCl_3$) δ 7.46 (m, 4 H), 7.33 (t, *J* = 7.5 Hz, 2H), 7.22 (m, 1H), 7.06 (d, *J* = 16.3 Hz, 1H), 6.95 (d, *J* = 16.3 Hz, 1H), 6.88 (d, *J* = 8.7 Hz, 2H), 3.97 (t, *J* = 6.5 Hz, 2H), 3.18 (t, *J* = 7.0 Hz, 2H), 1.79 (m, 4H), 1.43 - 1.31 (m, 8H).

(*E*)-4-(9-Iodononyloxy)stilbene (5h)

Obtained from **4h** according to METHOD D. Yield: 100%. M.p.: 100 °C. Rf (cyclohexane/ethyl acetate 9:1) = 0.74. ^{1}H NMR (300 MHz, $CDCl_3$) δ 7.46 (m, 4H), 7.34 (t, *J* = 7.5, 2H), 7.22 (m, 1H),

7.06 (d, *J* = 16.3 Hz, 1H), 6.96 (d, *J* = 16.3 Hz, 1H), 6.88 (d, *J* = 8.8 Hz 2H), 3.97 (t, *J* = 6.5 Hz, 2H), 3.19 (t, *J* = 7.0 Hz, 2H), 1.92 – 1.68 (m, 4H), 1.49 – 1.18 (m, 10H).

(*E*)-4-(10-Iododecyloxy)stilbene (5i)

Obtained from **4i** according to METHOD D. Yield: 100%. M.p.: 122 °C. Rf (cyclohexane/ethyl acetate 9:1) = 0.74. ^{1}H NMR (300 MHz, $CDCl_3$) δ 7.46 (m, 4H), 7.34 (t, *J* = 7.5 Hz, 2H), 7.22 (m, 1H), 7.06 (d, *J* = 16.4 Hz, 1H), 6.96 (d, *J* = 16.4 Hz, 1H), 6.92 – 6.85 (m, 2H), 3.97 (t, *J* = 6.5 Hz, 2H), 3.19 (t, *J* = 7.0 Hz, 2H), 1.88 – 1.70 (m, 4H), 1.51 – 1.22 (m, 12H).

(*E*)-3',5'-Dimethoxy-4-(2-triethylammoniumethyloxy)stilbene iodide (PtN-2)

Obtained from **3a** according to METHOD E. Yield: 89%. M.p.: 169 °C. ^{1}H NMR (300 MHz, DMSO) δ 7.56 (d, *J* = 8.7 Hz, 2H), 7.22 (d, *J* = 16.4 Hz, 1H), 7.02 (m, 3H), 6.73 (d, *J* = 2.2 Hz, 2H), 6.38 (t, *J* = 2.2 Hz, 1H), 4.40 (t, *J* = 4.6 Hz, 2H), 3.76 (s, 6H), 3.67 (t, *J* = 4.6 Hz, 2H), 3.37 (q, *J* = 7.1 Hz, 6H), 1.22 (t, *J* = 7.1 Hz, 9H). ^{13}C NMR (75 MHz, DMSO) δ 161.11, 157.55, 139.75, 130.90, 128.79, 128.29, 127.11, 115.35, 104.69, 100.04, 61.51, 55.66, 53.37, 7.76.

(*E*)-3',5'-Dimethoxy-4-(4-triethylammoniumbutyloxy)stilbene iodide (PtN-4)

Obtained from **3c** according to METHOD E. Yield: 92%. M.p.: 138°C. ^{1}H NMR (300 MHz, MeOD) δ 7.54 – 7.43 (m, 2H), 7.10 (d, *J* = 16.3 Hz, 1H), 7.01 – 6.86 (m, 3H), 6.69 (d, *J* = 2.2 Hz, 2H), 6.37 (t, *J* = 2.2 Hz, 1H), 4.05 (t, *J*= 5.4 Hz, 2H), 3.79 (s, 6H), 3.37 – 3.25 (m, 8H), 1.85 (m, 4H), 1.26 (t, *J* = 7.4, 9H). ^{13}C NMR (75 MHz, MeOD) δ 161.12, 158.53, 139.74, 130.20, 128.27, 127.60, 126.29, 114.44, 103.96, 99.13, 66.56, 56.24, 54.49, 52.57, 25.59, 18.30, 6.47.

(*E*)-4-(4-Triethylammoniumbutyloxy)stilbene iodide (StN-4)

Obtained from **5c** according to METHOD E. Yield: 92%. M.p.: 159 °C. ^{1}H NMR (300 MHz, DMSO) δ 7.57 – 7.49 (m, 4H), 7.34 (t, *J* = 7.6 Hz, 2H), 7.26 – 7.13 (m, 2H), 7.07 (d, *J* = 16.4 Hz, 1H), 6.95 (d, *J* = 8.7 Hz, 2H), 4.03 (m, 2H), 3.23 (m, 8H), 1.76 (m, 4H), 1.16 (t, *J* = 7.0 Hz, 9H).

^{13}C NMR (75 MHz, DMSO) δ 158.58, 137.78, 130.24, 129.12, 128.82, 128.44, 128.26, 127.67, 126.63, 126.61, 115.20, 67.10, 56.08, 52.53, 52.49, 52.45, 46.24, 25.86, 18.41, 7.62.

(*E*)-4-(6-Triethylammoniumhexyloxy)stilbene iodide (StN-6)

Obtained from **5e** according to METHOD E. Yield: 81%. M.p.: 166 °C. ^{1}H NMR (300 MHz, $CDCl_3$) δ 7.52 – 7.38 (m, 4H), 7.33 (t, *J* = 7.6 Hz, 2H), 7.24 – 7.18 (m, 1H), 7.05 (d, *J* = 16.5 Hz, 1H), 6.95 (d, *J* = 16.5 Hz, 1H), 6.88 (d, *J* = 7.3 Hz, 2H), 3.99 (t, *J* = 6.0 Hz, 2H), 3.44 (q, *J* = 7.0 Hz, 6H), 3.34 – 3.22 (m, 2H), 1.94 – 1.67 (m, 4H), 1.57 – 1.48 (m, 4H), 1.39 (t, *J* = 7.0 Hz, 9H).

^{13}C NMR (75 MHz, $CDCl_3$) δ 158.72, 137.58, 130.03, 128.67, 128.16, 127.77, 127.25, 126.57, 126.24, 114.82, 67.65, 57.77, 53.85, 28.98, 26.22, 25.69, 22.21, 8.36.

(*E*)-4-(8-Triethylammoniumoctyloxy)stilbene iodide (StN-8)

Obtained from **5g** according to METHOD E. Yield: 75%. M.p.: 163 °C.

^{1}H NMR (300 MHz, $CDCl_3$) δ 7.53 – 7.38 (m, 4H), 7.33 (t, *J* = 7.6 Hz, 2H), 7.25 – 7.17 (m, 1H), 7.05 (d, *J* = 16.4 Hz, 1H), 6.95 (d, *J* = 16.4 Hz, 1H), 6.87 (d, *J* = 8.8 Hz, 2H), 3.95 (t, *J* = 6.4 Hz, 2H), 3.44 (q, *J* = 7.2 Hz, 6H), 3.31 – 3.19 (m, 2H), 1.84 – 1.58 (m, 4H), 1.53 – 1.27 (m, 17H).

^{13}C NMR (75 MHz, $CDCl_3$) δ 158.84, 137.62, 129.95, 128.64, 128.21, 127.70, 127.20, 126.50, 126.21, 114.76, 67.91, 57.80, 53.82, 29.12, 29.04, 26.37, 25.83, 22.21, 8.32.

(*E*)-4-(3-Triphenylphosphoniumpropyloxy)stilbene iodide (StP-3)

Obtained from **5b** according to METHOD F. Yield: 72%. M.p.: 107 °C. ^{1}H NMR (300 MHz, $CDCl_3$) δ 7.96 – 7.62 (m, 15H), 7.55 – 7.31 (m, 6H), 7.27 – 7.19 (m, 1H), 7.04 (d, *J* = 16.3 Hz, 1H), 6.95 (d, *J* = 16.3 Hz, 1H), 6.91 – 6.82 (m, 2H), 4.35 (t, *J* = 5.7 Hz, 2H), 4.03 – 3.87 (m, 2H), 2.30 – 2.13 (m, 2H).

^{13}C NMR (75 MHz, CDCl3) δ 157.78, 137.55, 135.20, 135.17, 133.79, 133.69, 130.67, 130.50, 128.65, 128.09, 127.77, 127.26, 126.81, 126.26, 118.57, 117.42, 114.92, 66.71, 66.49, 22.90, 22.86, 20.37, 19.67.

(*E*)-4-(4-Triphenylphosphoniumbutyloxy)stilbene iodide (StP-4)

Obtained from **5c** according to METHOD F. Yield: 80%. M.p.: 109 °C. ^{1}H NMR (300 MHz, $CDCl_3$) δ 7.91 – 7.60 (m, 15H), 7.54 – 7.27 (m, 6H), 7.27 – 7.17 (m, 1H), 7.03 (d, *J* = 16.3 Hz, 1H), 6.94 (d, *J* = 16.3 Hz, 1H), 6.87 – 6.76 (d, *J* = 8.7 Hz, 2H), 4.08 (t, *J* = 5.6 Hz, 2H), 3.84 – 3.68 (m, 2H), 2.21 (p, *J* = 6.4 Hz, 2H), 1.98 – 1.79 (m, 2H). ^{13}C NMR (75 MHz, CDCl3) δ 158.36, 137.55, 135.18,

135.16, 135.14, 133.75, 130.65, 130.49, 130.22, 128.10, 127.75, 127.25, 126.67, 126.23, 118.59, 117.45, 114.73, 66.47, 29.38, 29.16, 22.76, 22.09, 19.36, 19.31.

(*E*)-4-(5-Triphenylphosphoniumpentyloxy)stilbene iodide (**StP-5**)

Obtained from **5d** according to METHOD F. Yield: 92%. M.p.: 99°C. ^{1}H NMR (300 MHz, DMSO) δ 7.94 – 7.68 (m, 15H), 7.58 – 7.45 (m, 4H), 7.34 (t, *J* = 7.6 Hz, 2H), 7.27 – 7.12 (m, 2H), 7.06 (d, *J* = 16.4 Hz, 1H), 6.85 (d, *J* = 8.7 Hz, 2H), 3.93 (t, *J* = 6.0 Hz, 2H), 3.62 – 3.54 (m, 2H), 1.72 (m, 2H), 1.60 (m, 4H). ^{13}C NMR (75 MHz, DMSO) δ 158.71, 137.80, 135.37, 135.33, 134.12, 133.99, 130.79, 130.63, 130.04, 129.11, 128.47, 128.26, 127.63, 126.61, 126.50, 119.55, 118.42, 115.09, 67.69, 28.25, 27.22, 27.00, 22.09, 21.02, 20.36.

(*E*)-4-(6-Triphenylphosphoniumhexyloxy)stilbene iodide (**StP-6**)

Obtained from **5e** according to METHOD F. Yield: 89%. M.p.: 88 °C. ^{1}H NMR (300 MHz, $CDCl_3$) δ 7.90 – 7.63 (m, 15H), 7.50 – 7.36 (m, 4H), 7.33 (t, *J* = 7.4 Hz, 2H), 7.25 – 7.16 (m, 1H), 7.04 (d, *J* = 16.4 Hz, 1H), 6.94 (d, *J* = 16.4 Hz, 1H), 6.88 – 6.79 (d, *J* = 8.8 Hz, 2H), 3.93 (t, *J* = 6.2, 2H), 3.76 (m, 2H), 1.71 (m, 6H), 1.48 (m, 2H). ^{13}C NMR (75 MHz, DMSO) δ 158.79, 137.81, 135.38, 135.33, 134.13, 133.99, 130.79, 130.63, 130.00, 129.12, 128.49, 128.26, 127.64, 126.61, 126.49, 119.58, 118.45, 115.10, 67.76, 30.13, 29.90, 28.78, 25.21, 22.22, 20.97, 20.31.

(*E*)-4-(7-Triphenylphosphoniumheptyloxy)stilbene iodide (**StP-7**)

Obtained from **5f** according to METHOD F. Yield: 89%. M.p.: 76 °C. ^{1}H NMR (300 MHz, $CDCl_3$) δ 7.91 – 7.76 (m, 9H), 7.76 – 7.64 (m, 6H), 7.52 – 7.39 (m, 4H), 7.34 (t, *J* = 7.5 Hz, 2H), 7.26 – 7.18 (m, 1H), 7.05 (d, *J* = 16.3 Hz, 1H), 6.95 (d, *J* = 16.3 Hz, 1H), 6.85 (d, *J* = 8.8 Hz, 2H), 3.93 (t, *J* = 6.4 Hz, 2H), 3.80 – 3.65 (m, 2H), 1.81 – 1.66 (m, 6H), 1.48 – 1.29 (m, 4H). ^{13}C NMR (75 MHz, DMSO) δ 158.82, 137.81, 135.36, 135.32, 134.11, 133.98, 130.79, 130.62, 129.96, 129.28, 129.11, 128.49, 128.25, 127.62, 126.60, 126.45, 119.58, 118.45, 115.09, 67.80, 30.32, 30.10, 28.94, 28.27, 25.65, 22.18, 22.13, 20.95, 20.29.

(*E*)-4-(8-Triphenylphosphoniumoctyloxy)stilbene iodide (**StP-8**)

Obtained from **5g** according to METHOD F. Yield: 86%. M.p.: 80 °C. ^{1}H NMR (300 MHz, $CDCl_3$) δ 7.89 – 7.74 (m, 9H), 7.74 – 7.65 (m, 6H), 7.52 – 7.38 (m, 4H), 7.33 (t, *J* = 7.5 Hz, 2H), 7.27 – 7.16 (m, 1H), 7.05 (d, *J* = 16.3 Hz, 1H), 6.94 (d, *J* = 16.3 Hz, 1H), 6.85 (d, *J* = 8.8 Hz, 2H), 3.93 (t, *J* = 6.5 Hz, 2H), 3.78 – 3.63 (m, 2H), 1.78 – 1.66 (m, 6H), 1.47 – 1.25 (m, 6H). ^{13}C NMR (75 MHz, $CDCl_3$) δ 158.83, 137.63, 135.17, 135.13, 133.70, 133.57, 130.66, 130.50, 129.84, 128.61, 128.24, 127.66, 127.15, 126.39, 126.19, 118.65, 117.51, 114.71, 67.94, 30.43, 30.23, 29.09, 29.01, 28.87, 25.82, 23.44, 22.77, 22.60, 22.54.

(*E*)-4-(9-Triphenylphosphoniumnonyloxy)stilbene iodide (StP-9)

Obtained from **5h** according to METHOD F. Yield: 91%. M.p.: 72 °C. ^{1}H NMR (300 MHz, $CDCl_3$) δ 7.83 – 7.72 (m, 9H), 7.72 – 7.62 (m, 6H), 7.48 – 7.34 (m, 4H), 7.30 (t, *J* = 7.5 Hz, 2H), 7.18 (m, 1H), 7.01 (d, *J* = 16.3 Hz, 1H), 6.91 (d, *J* = 16.3 Hz, 1H), 6.84 (d, *J* = 8.7 Hz, 2H), 3.91 (t, *J* = 6.5 Hz, 2H), 3.59 (m, 2H), 1.79 – 1.51 (m, 6H), 1.45 – 1.12 (m, 8H). ^{13}C NMR (75 MHz, CDCl3) δ 158.86, 137.63, 135.17, 135.13, 133.70, 133.57, 130.66, 130.50, 129.84, 128.61, 128.24, 127.67, 127.14, 126.38, 126.19, 118.65, 117.51, 114.71, 68.01, 30.48, 30.28, 29.15, 29.13, 29.04, 29.01, 25.89, 23.45, 22.79, 22.59, 22.53.

(*E*)-4-(10-triphenylphosphoniumdecyloxy)stilbene iodide (StP-10)

Obtained from **5i** according to METHOD F. Yield: 87%. M.p.: 67 °C. ^{1}H NMR (300 MHz, $CDCl_3$) δ 7.90 – 7.74 (m, 9H), 7.79 – 7.63 (m, 6H), 7.53 – 7.38 (m, 4H), 7.33 (t, *J* = 7.5 Hz, 2H), 7.31 – 7.17 (m, 1H), 7.06 (d, *J* = 16.3 Hz, 1H), 6.95 (d, *J* = 16.3 Hz, 1H), 6.88 (d, *J* = 8.7 Hz, 2H), 3.95 (t, *J* = 6.5 Hz, 2H), 3.73 (m, 2H), 1.82 – 1.60 (m, 6H), 1.42 (m, 2H), 1.25 (m, 8H). ^{13}C NMR (75 MHz, $CDCl_3$) δ 158.87, 137.64, 135.18, 135.14, 133.72, 133.59, 130.67, 130.50, 129.84, 128.63, 128.53, 128.43, 128.25, 127.68, 127.16, 126.38, 126.20, 118.67, 117.53, 114.71, 68.03, 30.54, 30.34, 29.36, 29.24, 29.20, 29.13, 29.12, 29.09, 25.94, 23.46, 22.80, 22.62, 22.56.

Biological Assays

Chemicals and drugs

Nicotine and αBungarotoxin were purchased from Tocris Bioscience (Bristol, UK). All of the other reagents (PMSF, protease inhibitors, acetylcholine chloride, atropine, bovine serum albumin, Cyclosporin A chemicals) were from Sigma-Aldrich (Italy).

Cell cultures

The Human U87MG glioblastoma cell line was kindly provided by Dr. Antonio Daga (IRCSS – San Martino Hospital, Genoa, Italy). The SH-SY5Y human neuroblastoma and A549 human lung adenocarcinoma cells were obtained from American Type Culture Collection (ATCC, USA). The U87MG and HEK cells were grown in high glucose Dulbecco's modified Eagle medium (DMEM) (Gibco, Invitrogen, Italy) supplemented with 10% Fetal Bovine Serum, (FBS) (Carlo Erba, Italy), 2 mM L-glutamine, and 1% penicillin-streptomycin (Euroclone, Italy). The SH-SY5Y and A549 cell lines were grown in RPMI 1640 (Lonza, Italy), supplemented with 10% FBS, 2 mM L-glutamine, 1% penicillin-streptomycin. The cells were maintained in a 5% CO_2 environment at 37°C.

Mouse astrocytes were maintained in minimum essential medium containing Earle's salts and 25 mM Hepes supplemented with 10% FBS, 0. 6% glucose, 1 mM Na piruvate, 200 mM glutamine and 1% penicillin-streptomycin.

The HepG2 cell line was bought from ATCC (HB-8065, ATCC from LGC Standards, Milan, Italy) and was cultured in Dulbecco's Modified Egle Medium (DMEM) high glucose with stable L-glutamine, supplemented with 10% Fetal Bovine Serum (FBS), 100 U/mL penicillin, 100 µg/mL streptomycin (complete growth medium) with incubation at 37 °C under 5% CO_2 atmosphere. HepG2 cells were used for no more than 20 passages after thawing, because the increase in number of passages may change the cell characteristics and impair assay results.

Cell uptake of StN-2, StN-4 , StN-8 , and StP-8 compounds

A total of 3 x 10^4 HepG2 cells/well were seeded in black with clear bottom 96-well plates and kept in complete growth medium for one day before treatment. On the second day, cells were treated with 1.0, 10.0, 50.0, and 100.0 µM **StN-2** or vehicle (DMSO, blank samples) for 6 and 24 h, respectively.

In parallel, cells were treated with 1.0 μM **StN-4**, **StN-8**, and **StP-8** or vehicle (DMSO, blank samples) for 1, 6 and 24 h, respectively, in comparison with **StN-2** as reference compounds. At the end of the treatment period, the culture medium was discarded and cells were washed three times with 100.0 μl PBS. At the end of the last wash step, 100.0 μl of fresh PBS was added. The degree of each compound-uptake at intracellular level was measured exploiting the natural fluorescence of each compound (excitation/emission wavelengths 260/350 nm, respectively), using the Synergy H1 fluorescent plate reader from Biotek. Afterwards, PBS was removed and 100.0 μl of propidium iodide at a final concentration of 20 μl/ml was added for 10 min at RT. Then, propidium iodide solution was discarded and cells washed three times with 100.0 μl PBS. The fluorescence signals of the propidium iodide, which stained the HepG2 cell nuclei, were read using the Synergy H1 fluorescent plate reader from Biotek (excitation/emission wavelengths 535/620 nm, respectively). To calculate the degree of each compound uptake, fluorescence signals were normalized using the nuclei fluorescence signals (Relative Fluorescence Unit (RFU) 350/620 nm) and the normalized RFU of the blank samples were subtracted at each normalized RFU of treated samples.

Affinity of the compounds to α7 and α4β2 nicotinic receptors

Affinity of the compounds for α7 and α4β2 nicotinic receptors

The affinity (Ki) of the compounds was determined by means of binding studies using the α7 and α9 specific ligand αBungarotoxin and SH-SY5Y cells transfected with cDNA encoding human α7 subunit. The Ki of the compounds for the α4β2 subtype was determined using the ligand (±)-[^{3}H]epibatidine and HEK293 cells transfected with the human α4 and β2 pcDNAs. The SH-SY5Y and HEK 293 cells were transfected at 30% confluency, and the cells were maintained at 37°C in an environment containing 5% $CO_{2\ as}$ previously described .[23]

The cell transfections were carried out in 100 mm Petri dishes using 18 μL JetPEI^{TM} (Polypus, France) (1 mg/ml, pH 7.2) and 6 μg of pcDNAs diluted in NaCl 150 mM. After 48 h transfection, the cells were collected, washed with PBS by centrifugation and frozen.

[^{125}I]-αBungarotoxin (specific activity 100-120 Ci/mmol, radiolabeled by us using Na^{125}I and (±)-[^{3}H]epibatidine 60 Ci/mmol were purchased from Perkin-Elmer, (Boston, USA) and were used for the saturation and competition experiments. In order to determine [^{125}I]-**α**Bungarotoxin binding saturation experiments were performed by incubating α7- SH-SY5Y membranes overnight with 0.1-10 nM concentrations of [^{125}I]-αBungarotoxin at room temperature (RT). Nonspecific binding was determined in parallel by means of incubation in the presence of 1 **μ**M unlabelled **α**-Bungarotoxin. To determine (±)-[^{3}H]epibatidine binding, saturation experiments were performed by incubating aliquots of membranes from HEK cells expressing human α4β2 nAChRs with 0.01-2.5 nM concentrations of (±)-[^{3}H]epibatidine overnight at 4°C. Nonspecific binding was determined in parallel by incubation in the presence of 100 nM unlabelled epibatidine. After incubation, the samples were filtered and the bound radioactivity directly counted in a **γ** counter ([^{125}I]-**α**Bungarotoxin) or β counter ((±)-[^{3}H]epibatidine).

The inhibition of [^{125}I]-**α**-Bungarotoxin or (±)-[^{3}H]epibatidine binding by the test compounds was measured by pre-incubating the membranes of transfected α7- SH-SY5Y or HEK-α4β2 cells with increasing concentrations (10 pM to 10 mM) of the tested compound for 30 min at RT, followed by overnight incubation with a final concentration of 1 nM [^{125}I]-α-Bungarotoxin at RT or 0.25 nM (±)-[^{3}H]epibatidine at 4°C. [24]

The data from the competition binding assays were evaluated using one-site competitive binding curve-fitting procedures and GraphPad Prism version 6 (GraphPad Software, Inc, CA, USA). Inhibition constants (Ki_s) were estimated by fitting three independent competition binding experiments and the Kd of the radioligands, according to the Cheng-Prusoff equation.

Two-electrode voltage clamp recording of α7- and α9α10-nAChR function

Xenopus laevis oocytes were used to heterologously express cloned human nAChR subtypes. The tips of pulled glass micropipettes were broken to achieve an outer diameter of ~40 μm (resistance of 2-6 MΩ), and pipettes were used to inject fifty nL (20-30 ng) of cRNA into each *Xenopus* oocyte with a Drummond microdispenser (Drummond Scientific, Broomall, PA, USA) and incubated at

17°C in ND96 (96.0 mM NaCl, 2.0 mM KCl, 1.8 mM $CaCl_2$, 1.0 mM $MgCl_2$, and 5 mM HEPES, pH 7.5) containing antibiotics (100 U/mL penicillin G, 100 µg/mL streptomycin, 100 µg/mL gentamycin. One to five days after injection, *Xenopus* oocytes expressing nAChR subtypes were voltage clamped at −70 mV with an Warner Instruments OC-725 series amplifier amplifier (Warner Instruments, Hamden, CT) and exposed to acetylcholine (ACh), and compounds as described previously (Hone *et al.,* 2009). Briefly, the oocyte chamber consisting of a cylindrical well (~30 µL in volume) was gravity perfused at a rate of ~2 mL/min with ND-96 buffer supplemented with 0.1 mg mL^{-1} BSA. The oocyte was subjected once a minute to a 1 sec pulse of 10 µM ACh (α9α10 nAChR) or 200 µM ACh (α7 nAChR) The compounds were dissolved in ND96 and either perfusion-applied until equilibrium block was acheived (for concentrations of ≤1 µM) or applied in a static bath for 5 min during which the buffer flow was stopped (for concentrations of ≥10 µM).

Viability assay

Cell viability was assessed using the CellTiter 96® AQueous One Solution Cell Proliferation Assay (Promega, Italy) which is based on the reduction of water-soluble MTS tetrazolium salt by viable cells. The resulting formazan dye was quantified at an absorbance at 490 nm using Perkin Elmer Wallac 1420 Victor^2 Microplate Reader.

The cells depending on cell proliferation rate were plated in 24-well plates at different densities of each cell line: 15 x 10^3 U87MG and SH-SY5Y cells or 8 x 10^3 A549 cells or 50 x10^3 for the mouse astrocytes. The A549 cells were rendered quiescent by means of serum deprivation for 72 hours after which serum was added to the cultures and the cells exposed to drugs. Mouse astrocytes were rendered quiescent by reducing serum concentration of the growth medium from 10% to 2% ; the low serum percentage was kept for the entire treatment period. All of the tumoral and control glial cells were incubated with increasing concentrations of the compounds for 72 hours starting the day after plating. Complete medium with desired compound was refreshed once a day. After 72 h of compound exposure, the cells were washed with PBS, fresh medium was added, and 50 µl of the MTS solution

was pipetted into each well and depending on the metabolic activity the cells were incubated between 30 minutes and two hours at 37°C.

The absorbance of the control cells (not treated with the compounds) in the MTS assays was assumed to be 100%. The drug-induced decrease in viability was calculated as a percentage of that of the untreated control cells. Each sample was tested in triplicate, and each assay was made in four-six independent experiments.

The IC_{50} values were derived from a non linear regression model based on a dose response curve (variable slope) fitted by a non linear linear regression analysis made using the Prism 6 programme.

ATP assay

ATP concentrations were determined using a luciferin-luciferase method. Briefly, 10^6cells/treatment were resuspended in buffer-A (150 mM KCl, 25 mMTris-HCl, 2 mM EDTA, 0.1% BSA, 10 mM potassium phosphate and 0.1 mM $MgCl_2$ (pH 7.4)) and incubated for 1 min with digitonin (10 μg/10^6 cells) at room temperature with gentle agitation. The cells were distributed and plated in 96 wells $2x10^5$cells/well. The samples were treated with a mix containing 2 mM malate, 1 mM pyruvate, 1 mM ADP and buffer-B (containing 0.2 mM luciferin and 5 μg/ml luciferase in 0.5 M Tris-acetate (pH 7.75). Oligomycin (2 μg/ml) was also added to detect glycolytic ATP ATP was measured using a GloMax luminometer (Promega, Madison, WI, USA).

Mitochondrial ROS detection

U87MG cells were seeded in 6-well plates at a density of 4 x 10^5 cells/well and on the following day were incubated for 10 minutes with a solution of 1 μM MitoSOX Red Mitochondrial Superoxide Indicator (Thermofisher, Italy) plus 2 μM Cyclosporin A or 100 nM tetramethylrhodamine methyl ester perchlorate (TMRM), (Thermofisher, Italy) plus 2 μM Cyclosporin A dissolved in complete growth medium. Control cells were incubated with Cyclosporin A alone. The compounds were added at the desired concentrations and the cells incubated at 37°C for one hour, and then trypsinised, washed and resuspended with 500 μl of HBSS with calcium and magnesium.

In each experiment the positive control were the cells treated 50 μM Antimycin A (Sigma, Italy).

The fluorescence signal was assessed using BD FACSCAlibur flow cytometer, a 488 nm argon-ion laser as an excitation source, a 585 nm band pass filter, and a photomultiplier as detector of fluorescence emission.

Data and statistical analyses

The data from the binding, cell viability, ATP and ROS production experiments were expressed as mean values ± SEM and analysed by means of a Student's *t* test for comparisons of two groups, or one-way ANOVA followed by a Bonferroni *post hoc* test (paramatric data) or by Kruskal–Wallis test followed by Dunn's *post hoc* test for non-parametric data. The accepted level of significance was $P<0.05$. All of the statistical analyses were made using Prism software, version 6 (GraphPad).

Acknowledgements. Drs Susanna Pucci, Francesca Fasoli and Irene Corradini are recipients of fellowships from Fondazione Vollaro, Milan. We thanks prof Michela Matteoli for the astrocytes gift. This work was supported by the Università degli Studi of Milan, the CNR Research Projects Aging, PRONAT and InterOmics, grants from Fondazione Monzino (Milan) and from Fondazione Vollaro (Milan) and from NIH grants GM103801 and GM48677 to JMM.

Supporting information. The Supporting Information is available free of charge on the ACS Publications website at DOI: UNKNOWN.

Molecular Formular Strings (.CSV)

^{1}H NMR and ^{13}C NMR spectra of synthesized compounds tested pharmacologically

Elemental analysis data of synthesized compounds tested pharmacologically (Table S1)

REFERENCES

(1) Neuzil, J.; Dong, L. F.; Rohlena, J.; Truksa, J.; Ralph, S. J. Classification of mitocans, anti-canver drugs acting on mitochondria. *Mitochondrion* **2013**, *13*, 199-208.

(2) Mattarei, A.; Romio, M.; Managò, A.; Zoratti, M.; Paradisi, C.; Szabò, I.; Leanza, L.; Biasutto, L. Novel mitochondria-targeted furocoumarin derivatives as possible anti-cancer agents. *Front. Oncol.* **2018**, *8*, article 122.

(3) Ueda, S.; Masutani, H.; Nakamura, H.; Tanaka, T.; Ueno, M.; Yodoi, J. Redox control of cell death. *Antioxid. Redox Signal.* **2002**, *4*, 405-414.

(4) Murphy, M. P. Targeting lipophilic cations in mitochondria. *Biochim. Biophys. Acta* **2008**, *1777*, 1028-1031.

(5) Dong, L. F.; Jameson, V. J. A.; Tilly, D.; Cerny, J.; Mahdavian, E.; Marin-Hernandez, A.; Hernandez-Esquivel, L.; Rodriguez-Enriquez, S.; Witting, P. K.; Stantic, B.; Rohlena, J.; Truksa, J.; Kluckova, K.; Dyason, J. C.; Salvatore, B. A.; Moreno-sanchez, R.; Coster, M. J.; Ralph, S. J.; Smith, R. A. J.; Neuzil, J. Mitochondrial targeting of vitamin E succinate enhances its pro-apoptotic and anti-cancer activity via mitochondrial complex II. *J. Biol. Chem.* **2011**, *286*, 3717-3728.

(6) Mattarei, A.; Biasutto, L.; Rastrelli, F.; Garbisa, S.; Marotta, E.; Zoratti, M.; Paradisi, C. Regioselective O-derivatization of quercetin via ester intermediates. An improved synthesis of rhamnetin and development of a new mitochondriotropic deirivative. *Molecules* **2010**, *15*, 4722-4736.

(7) Sassi, N.; Mattarei, A.; Azzolini, M.; Bernardi, P.; Szabò, I.; Paradisi, C.; Zoratti, M.; Biasutto, L. Mitochondria-targeted resveratrol derivatives acta s cytotoxic pro-oxidants. *Curr. Pharm. Design* **2014**, *20*, 172-179.

(8) Gotti, C.; Balestra, B.; Moretti, M.; Rovati, G. E.; Maggi, L.; Rossoni, G.; Berti, F.; Villa, L.; Pallavicini, M.; Clementi, F. 4-Oxystilbene compounds are selective ligands for neuronal nicotinic αBungarotoxin receptors. *Br. J. Pharmacol.* **1998**, *124*, 1197-1206.

(9) Zoli, M.; Pistillo, F.; Gotti, C. Diversity of native nicotinic receptor subtypes in mammalian brain. *Neuropharmacol.* **2015**, *96*, 302-311.

(10) Zoli, M.; Pucci, S.; Vilella, A.; Gotti, C. Neuronal and extraneuronal nicotinic acetylcholine

(11) Grando, S. A. Connection of nicotine to cancer. *Nat. Rev. Cancer* **2014**, *14*, 419-429.

(12) Mucchietto, V.; Crespi, A.; Fasoli, F.; Clementi, F.; Gotti, C. Neuronal acetylcholine nicotinic receptors as new targets for lung cancer treatment. *Curr. Pharm. Des.* **2016**, *22*, 2160-2169.

(13) Mucchietto, V.; Fasoli, F.; Pucci, S.; Moretti, M.; Benfante, R.; Maroli, A.; Di Lascio, S.; Bolchi, C.; Pallavicini, M.; Dowell, C.; McIntosh, M.; Clementi, F.; Gotti, C. α9 and α7-containing receptors mediate the proproliferative effects of nicotine in the A549 adenocarcinoma cell line. *Br. J. Pharmacol.* **2018**, *175*, 1957-1972.

(14) Rohlena, J.; Dong, L. F.; Kluckova, K.; Zobalova, R.; Goodwin, J.; Tilly, D.; Stursa, J.; Pecinova, A.; Philimonenko, A.; Hozak, P.; Banerjee, J.; Ledvina, M.; Sen, C. K.; Houstek, J.; Coster, M. J.; Neuzil, J. Mitochondrially targeted α.tocopheryl succinate is antiangiogenic: potential benefit against tumor angiogenesis but caution against wound healing. *Antioxid. Redox Signal.* **2011**, *15*, 2923-2935.

(15) Schweizer, E. E.; Bach, R. D. Phosphonium salts. II. 2-Bromophenetole and triphenylphosphorus as novel phosphonioethylation precursors. *J. Org. Chem.* **1964**, *29*, 1746-1751.

(16) Sassi, N.; Mattarei, A.; Azzolini, M.; Szabo, I.; Paradisi, C.; Zoratti, M.; Biasutto, L. Cytotoxicity of mitochondria-targeted resveratrol deivatives: interactions with respiratory chain complexes and ATP synthase. *Biochim. Biophys. Acta* **2014**, *1837*, 1781-1789.

(17) Fasoli, F.; Mucchietto, V.; Benfante, R.; Maroli, A.; Tamburini, M.; Matteoli, M.; Clementi, F.; Gotti, C. Pharmacological characterization of nicotinic acetylcholine receptors expressed in glioma and glioblastoma cell. Poster C113, FENS 2016, Copenhagen.

(18) Benfante, R.; Antonini, R. A.; De Pizzol, M.; Gotti, C.; Clementi, F.; Locati, M.; Fornasari, D. Expression of the alpha7 nAChR subunit duplicate form (CHRFAM7A) is down-regulated in the monocytic cell line THP-1 on treatment with LPS. *J. Neuroimmunol.* **2011**, *230*, 74-84.

(19) Weber, G. F. Time and circumstances: cancer cell metabolism at various stages of disease progression. *Front. Oncol.* **2016**, *6*, article 257.

(20) Dong, L. F.; Jameson, V. J. A.; Tilly, D.; Prochazka, L.; Rohlena, J.; Valis, K.; Truksa, J.; Zobalova, R.; Mahdavian, E.; Kluckova, K.; Stantic, M.; Stursa, J.; Freeman, R.; Witting, P. K.; Norberg, E.; Goodwin, J.; Salvatore, B. A.; Novotna, J.; Turanek, J.; Ledvina, M.; Hozak, P.; Zhivotovsky, B.; Coster, M. J.; Ralph, S. J.; Smith, R. A. Moreno-sanchez, R.; Coster, M. J.; Ralph, S. J.; Smith, R. A. J.; Neuzil, J. Mitochondrial targeting of α-tocopheryl succinate enhances its pro-apoptotic efficacy: a new paradigm for effective cancer therapy. *Free Radic. Biol. Med.* **2011**, *50*, 1546-1555.

(21) Biasutto, L.; Mattarei, A.; Marotta, E.; Bradaschia, A.; Sassi, N.; Garbisa, S.; Zoratti, M.; Paradisi, C. Development of mitochondria-targeted derivatives of resveratrol. *Bioorg. Med. Chem. Lett.* **2008**, *18*, 5594-5597.

(22) Wyrzykiewicz, E.; Wendzonka, M. Synthesis and physicochemical characterization of fluorescent (E)-2-stilbenoxyalkylthiouracils and isomer differentiation using EIMS. *J. Heterocyclic Chem.* **2004**, *41*, 177-186.

(23) Moretti, M.; Zoli, M.; George, A. A.; Lukas, R. J.; Pistillo, F.; Maskos, U.; Whiteaker, P.; Gotti, C. The novel alpha7beta2-nicotinic acetylcholine receptor subtype is expressed in mouse and human basal forebrain: biochemical and pharmacological characterization. *Mol. Pharmacol.* **2014**, *86*, 306-317.

(24) Pallavicini, M.; Bolchi, C.; Binda, M.; Cilia, A.; Clementi, F.; Ferrara, R.; Fumagalli, L.; Gotti, C.; Moretti, M.; Pedretti, A.; Vistoli, G.; Valoti, E. 5-(2-Pyrrolidinyl)oxazolidinones and 2-(2-pyrrolidinyl)benzodioxanes: synthesis of all the stereoisomers and alpha4beta2 nicotinic affinity. *Bioorg Med Chem Lett*, **2009**, *19*(3), 854-859.

Table of Contents Graphic